This is to certify that the

thesis entitled

CORROSION: STOCHATIC MODELLING OF THE INITIATION RATE AND DAMAGE ON CORROSION DAMAGE

presented by

Zhiyun Li

has been accepted towards fulfillment
of the requirements for

M.S. degree in Metallurgy

Robert Stevens

Major professor

Date 21 May 1987

CORROSION: STOCHASTIC MODELLING OF THE INITIATION RATE AND EFFECT ON CORROSION DAMAGE

by

ZHIYUN LI

A THESIS

Submitted to
Michigan State University
in partial fulfillment of the requirements
for the degree of

MASTER OF SCIENCE

Department of Metallurgy, Mechanics, And Materials Science

1987

ABSTRACT

CORROSION: STOCHASTIC MODELLING OF THE INITIATION RATE AND EFFECT ON CORROSION DAMAGE

by

ZHIYUN LI

Corrosion is a two-step process: initiation and propagation. An initiation-time distribution model determined experimentally, was found to follow a Gamma function. Parameters for two corrosion processes were determined. Using the initiation distribution with a modified rate equation $W = A (t - \tau)^{b}$, "long-time" probability-damage-exposure time diagram were projected with 5%, 50%, 95% confidence, similar to a fatigue P-S-N diagram.

ACKNOWLEDGEMENTS

First and foremost, I would like to thank my advisor, Professor R. W. Summitt, for his patient guidance and beneficial discussions in making this thesis a success. Also, I would like to express my deepest gratitude to my parents for their boundless love, encouragement and full support.

TABLE OF CONTENTS

LIST OF TABLES

LIST OF FIGURES

I INTRODUCTION

The results of corrosion experiments, which have been designed mainly to determine reaction kinetics, show wide variations, especially over short-time exposure. It is generally accepted that corrosion, like fatigue cracking and other cumulative damage processes, consists of two steps: (a) initiation, followed by (b) propagation. The initiation step, however, is generally ignored, hence its influence on experimental results is not known. Corrosion rates frequently are slow (mm/yr,etc), and if the kinetics are slow, it is possible that the initiation process also may be slow, thus the initiation times for three or five random samples may be widely separated and may contribute significantly to the observed dispersion of results.

This study examined the initiation distribution experimentally for two simple systems in relatively severe environments, and the results were used to develop probability distribution models. These models were used to project corrosion damage for extended exposures, and then they were extrapolated to less severe environments, and the results were compared with published test data. Finally, published literature data were analyzed, from the standpoint of sample variation, to infer initiation rates.

II THEORETICAL BACKGROUND AND LITERATURE REVIEW

1. KINETICS OF REACTIONS

The need to establish a relationship between corrosion weight losses (or pitting depth) and exposure time is obvious, in order to predict the performance of a material from a field test, as well as to assess the effect of environmental factors on materials.

A general corrosion damage equation has been proposed by several authors,

$$W = At^b. \qquad (1)$$

where M is corrosion loss (either penetration depth or weight loss),

t is exposure time, and

A and b are empirical constants and are functions of environmental conditions

Miller and coworkers [1] pointed out that the exponential b theoretically takes on the value of approximately 1/2, when corrosion is limited by the diffusion rate of the relevant species through a semi-permeable film of reaction products. This would be the case for most aluminum alloys. When the corrosion products

are flocculant or soluble and offer no protection, linear corrosion kinetics are observed and b = 1.

The above equation may be expanded in the following manner to account for the presence of pollutants in the environment, for example, SO_2 and Cl^-,

$$W = At^b(P_1, P_2). \quad (2)$$

where P_1 and P_2 are damage coefficients governed by the presence of pollutants in the atmosphere. The experimental results show that the maximum corrosion rate for the aluminum alloys were obtained in solutions which contained both salt and acids.

Godard [2] developed an equation for determining pitting depth,

$$D = C\ (t)^{1/3}. \quad (3)$$

Knotkova-Cermakova et al. [3] performed corrosion tests at nineteen corrosion stations in the North-Bohemian modern region. On the basis of the results of three years of the described program, they analyzed the dependence of corrosion on time with the use of the power function ($W = at^b$), the expanded power function ($W = at^{b+ct}$), and the power function passing into a linear and hyperbolic function [$W = a + bt - (ac/t + c)$]. The best correlation was attained for the hyperbolic function.

All the analyses above seems to give a fair representation of corrosion phanomena in many sites, but there are some problems predicting long-time damage, and extrapolating the damage to other environments.

Bragard and Bonnarens [4] tried to use the power function law to predict long-time behavior of a steel from short-time experimental data. Their experimental data resulted from a long-term program carried out at three sites in Belgium: Liege (industrial site), Ostende I (marine site, considerable salt mist and fog), and Ostende II (marine site, protected from the sea by a dune). For each steel, values of A and b were calculated from the weight losses after 1, 2, 3, and 4 years exposure. The two parameters then were used to predict the weight loss after 10 years. The predicted and actual 10-year values for weight losses are given in Table 1.

For Liege and Ostende II, the calculated values are generally underestimated. For Liege, the predicted and actual values are very close, while for Ostende II the agreement is poorer. For Ostende I, the calculated values are nearly always misleading. The law $M = At^b$ is valid in numerous cases only as far as deviations of ±10 percent or even ±30 percent are allowed.

For the sake of generalization and interpretation of this law, the relationship in logarithmic form was

Table 1 Experimental and Calculated 10-year Weight Loss. by Bragard and Bonnarens

Steel	Liège			Ostende I			Ostende II		
	Experimental	Calculated	Experimental / Calculated	Experimental	Calculated	Experimental / Calculated	Experimental	Calculated	Experimental / Calculated
1	13.8	13.5	1.02	31.8	32.6	0.98	33.9	28.9	1.17
2	32.2	31.6	1.02	. . .	191.7	. . .	. . .	69.6	. . .
3	26.4	25.0	1.06	70.5	59.6	1.18	57.6	35.3	1.63
4	16.8	16.2	1.04	34.2	44.2	0.77	28.4	22.0	1.29
5	17.0	16.7	1.02	32.8	33.7	0.97	34.8	33.0	1.05
6	15.6	14.8	1.05	28.0	32.7	0.86	29.1	26.7	1.09
7	27.5	27.7	0.99	. . .	156.3	. . .	. . .	81.0	. . .
8	18.3	17.5	1.05	41.9	115.1	0.36	36.3	37.6	0.97
9	8.1	8.6	0.94	65.3	45.3	1.44	21.8	20.0	1.09
10	7.2	7.6	0.95	39.1	24.4	1.60	20.3	17.4	1.17
11	16.3	16.0	1.02	33.2	28.6	1.16	26.5	23.2	1.14
12	15.9	14.9	1.07	53.9	29.1	1.85	29.9	29.4	1.02
13	23.7	22.3	1.06	. . .	250.0	. . .	. . .	115.6	. . .
14	16.2	15.1	1.07	36.8	38.8	0.95	36.3	30.4	1.19
15	10.8	11.2	0.96	20.2	18.1	1.12	22.6	20.3	1.11
16	8.5	8.5	1.00	63.5	60.7	1.05	25.0	24.0	1.04
17	8.8	9.6	0.92	46.9	39.1	1.20	23.1	22.7	1.02
18	15.9	15.2	1.05	52.3	37.3	1.40	24.6	23.9	1.03
19	16.1	15.4	1.05	49.4	47.4	1.04	28.7	27.4	1.05
20	25.3	21.4	1.18	78.4	93.5	0.84	57.2	47.3	1.21
21	16.5	15.4	1.07	31.9	26.4	1.21	30.5	23.7	1.29
22	16.6	16.1	1.03	29.4	28.9	1.02	33.7	29.2	1.15
23	15.5	12.8	1.21	45.0	36.5	1.23	20.4	18.4	1.11
24	19.6	19.1	1.03	33.5	30.4	1.10	29.9	22.5	1.33

expressed

$$\text{Log } W_y = k\text{Log } W_x + n. \quad (4)$$

where W_y is the weight loss after y years,

W_x is the weight loss after x years, and

k and n coefficients depend upon the site and the time periods x and y

A set of data were selected from the literature and calculated. All plots of Figures 1, 2, 3 show definitely that empirical relationships can be developed between the corrosion losses at different exposure times, but in a band, instead of a straight line. The width of the band for 3.5 or 5 years of data prediction is narrower than that for 1 year.

Mikhailovsky [16], based on the mechanism of nonstationary atmospheric corrosion, proposed quite definite physical-chemical interpretations, expressing the metal corrosion rate:

$$K = K_0 (1 - \theta). \quad (5)$$

where K_0 is the corrosion rate at the active surface,

θ is the fraction of the surface covered by the corrosion components having the protective properties.

At same time $\theta = b (K - K').$ (6)

where b is a coefficient, and

K' is the steady corrosion rate equal to the

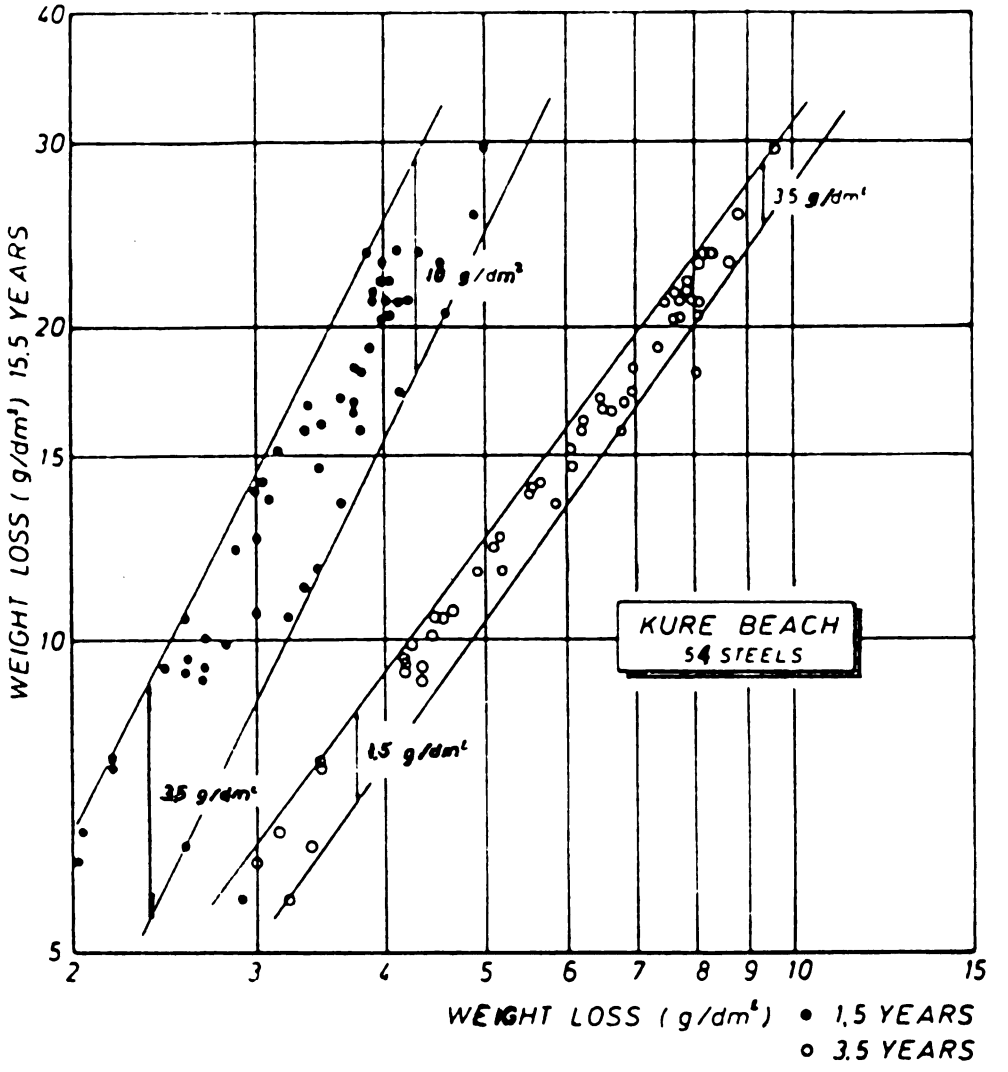

Figure 1. Relationship between short-term and long-term exposure periods, Kure Beach. by Bragard and Bonnarens

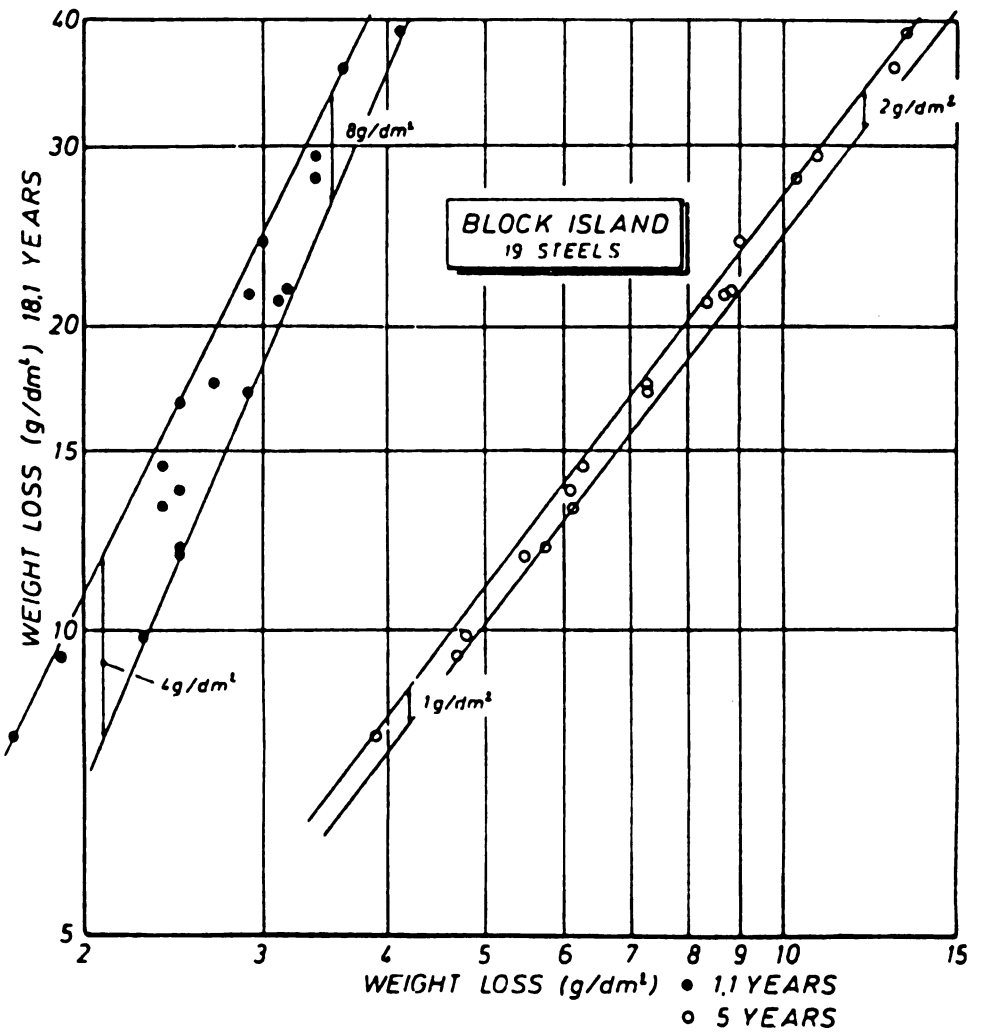

Figure 2. Relationship between short-term and long-term exposure periods, Block Island. by Bragard and Bonnarens

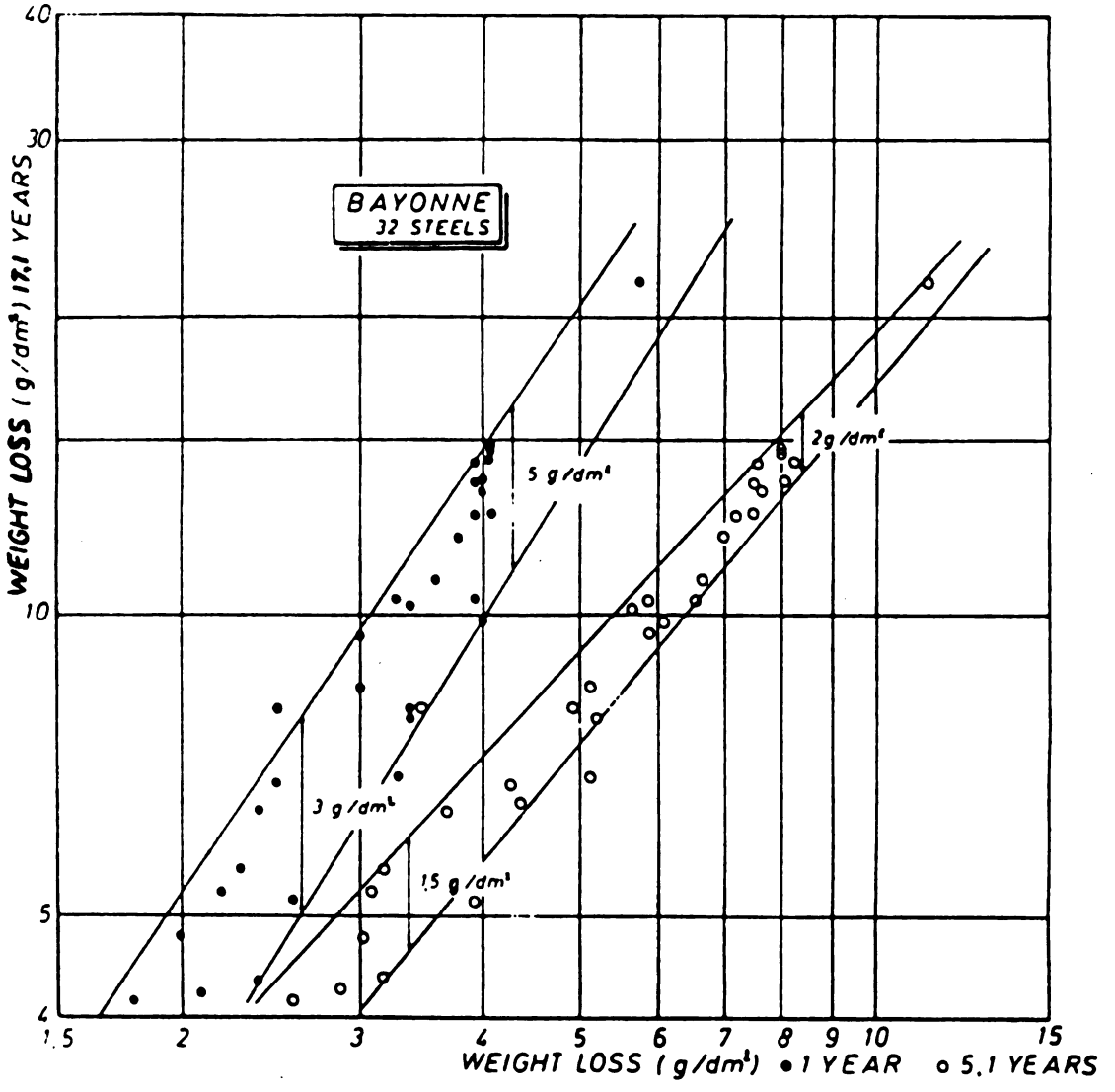

Figure 3. Relationship between short-term and long-term exposure periods, Bayonne. by Bragard and Bonnarens

protective surface layer damage rate under the action of environment medium.

Differentiation of Equations (5) & (6) with respect to time and solution of the differential equation system for K, yields

$$K = K_0 e^{-\beta\tau} + K' . \qquad (7)$$

$$W = (K_0/\beta) \quad (1 \; - \; e^{-\beta\tau} \;) + K' . \qquad (8)$$

where $\beta = K_0 b$, and

W = corrosive loss in time.

At the initiation time ($\tau = 0$), $K \rightarrow K_0$ (the maximum corrosion rate); when $\tau \rightarrow \infty$ the corrosion rate is stabilized and $K \rightarrow K'$. K, K_0, and K' are functions of the temperature-moisture and aerochemical atmospheric complex.

Metal corrosion in natural atmospheres should be considered as a combination of corrosive processes developed under adsorption and drop-liquid (phase) water film. Considering the effect of moisture and aerochemical air parameters on the rates of metal corrosion, the metal corrosion within the year (K_0) can be represented by

$$K_0 = K_{(ph)} \sum_{t_1}^{t_2} \sum^{n} \tau_{(ph)} + K_{(a)} \sum_{t_1}^{t_2} \sum^{n} \tau_{(a)}$$

where $K_{(ph)}$ and $K_{(a)}$ are the average metal corrosion rates under phase and adsorption water layers in $g/m^2/yr$

$\sum_{t_1}^{t_2} \sum^{n} \tau_{(ph)}$, $\sum_{t_1}^{t_2} \sum^{n} \tau_{(a)}$ are the total life time of

phase and of asorption water layers on metals in hr/year

Assuming that the mean corrosion $K_{(ph,a)}$ is proportional to the active impurities, then,

$$K_0 = [\ K^{(0)}_{(a,ph)} + B^{ch}_{(a,ph)} \cdot C^{ch}\ ] \sum_{t_1}^{t_2} \sum^{n} r_{(a,ph)}$$

where $K^{(0)}_{(a,ph)}$ is the corroson rate in the arbitrary pure atmosphere,

$B^{ch}_{a,ph}$ is the corrosion acceleration by the corrosion impurities in the air,

$C^{ch} \sum_{t_1}^{t_2} \sum^{n} r_{(a,ph)}$ is the quantitative property of air corrosive activity, and can be used for the standard atmospheric classification with respect to air corrosivity.

On calculating the temperature dependence of the metal corrosion rate in pure and polluted atmospheres, they developed a linear function,

$$K^{(0)}_{(ph)} = K^{(0)}_{(ph\ t=0)} + \alpha t \ (g/m^2/hr)$$

$K^{(0)}_{(ph\ t=0)}$ is the corrosion velocity at 0 °C

α is the temperature coefficient of the corrosion acceleration, and

t is the temperature.

The processing of experimental data obtained for $[C_{SO_2}] > 10\text{-}15$ mcg/m³ and $[Cl^-] > 1$ mg/m³ showed that the acceleration of steel corrosion $B^{(ch)}_{(ph)}$ caused by sulfur dioxide also depends on temperature and may be represented by

$$B^{(ch)}_{(ph)} = B^{(ch)}_{(ph,\ t=0)} + \gamma\ t\ (g/m^2\ hr/1\ mg/m^3\ SO_2)$$

where $B^{(ch)}_{(ph,\ t=0)}$ is the corrosion acceleration at 0 °C.

γ is the temperature coefficient of acceleration [$g/m^2(hr)/1mg/m^3\ SO_2/^oC$].

Thus the considered correlations between the metal corrosion rate and main meteorological and aerochemical properties of the atmosphere have strict physical-chemical bounds, and can be the basis for modeling and predicting he expected corrosion rate in different climatic regions.

As reported, the reliability of their corrosion parameters and the validity of their calculation method are supported by the comparison of calculated and actual data on the metal corrosion obtained in Ottawa and Cleveland. By using only the cited meteorological and aerochemical (containing SO_2) data, the expected rates for steel,

cooper, and zinc corrosion have been determined in those regions. The average calculation error was ∿16% for steel, ∿37% for copper, and ∿38% for zinc. The statistical analysis for calculation of the corrosion rates for five metals at the corrosion stations of COMECON countries showed that the calculation error does not exceed 18-20% with a probability of 0.95.

It can be concluded that there are disadvantages of the kinetic equation indicating there are some variables not accounted for, such as corrosion initiation, and hence damage cannot be predicted without taking probability into account.

2. CORROSION INITIATION

For dry atmospheric corrosion, it is believed that the mechanism of corrosion includes physical adsorption of molecular oxygen at the metal surface with a subsequent dissociaton to atomic oxygen and its chemisorption, formation of oxide nuclei at local regions on the surface-initiation, and formation and growth of a solid oxide film. In the case of moist atmospheric corroson, it includes adsorption (or sedimentation) water layer (oxygen donors) and ionizing components on the metal surface and interaction of corrosive gas molecules (or aerosol

particles) with adsorbed water molecules, and the formation of the electrolyte-chemical and electrochemical interaction of metals with the sorbed film.

Corrosion initiates at points of high Gibbs free energy. Metals are not ideal pure crystals, but are polycrystalline with impurities, various phases, slip planes, imperfections, minute flaws and manufacturing defects, having higher energies than those of the matrix, and corrosive species prefer to migrate to such sites. These variables can not be measured, their natures are unknown, and their distribution is random. Consequently, corrosion initiation is a stochastic process and must be treated statistically. The probability of initiation is a function of the environment, time and the nature of the materials, i.e.,

$$P = P\ (\text{environment, gormetry, material, time}). \quad (9)$$

Likewise, corrosion damage then would be the product of initiation time and propagation, i.e.,

$$D = PR. \quad (10)$$

where R is a kinetic rate equation. Thus, the problem is how to establish a general statistical model to describe the initiation.

Summitt [5] describes the frequency of corrosion initiation as a Poisson-Markov distribution process. With assumptions of non-overlapping intervals and independence

of failure, this will result in a Poisson distribution of failures and a Gamma distribution of times to failure.

Williams, Westcott and Fleischmann [6] developed a stochastic model for pitting initiation, involving as parameters an initiation frequency for pit nuclei, death probability for unstable pits, and a critical age which defines the transition between a stable and unstable pit. Results for the statistics of ensembles of current time transients of stainless steel are given.

They presented the induction time is a statistical variable; the survival probability for the specimen determined as a function of time showed Poisson distribution with a potential-dependent transient rate, and gave an equation of probability of a specimen remaining unpitted as a function of the exposure time and of the parameters of the model λ, μ and τ_c,

$$\text{Ln } [P(0)] = -\lambda a(t-\tau_c)\exp(-\mu\tau_s). \qquad (11)$$

where P(0) is the probability that no stable pitting is formed within time $t>\tau_c$,

τ_c is the critical age,

λ is the nucleation frequency, and

μ is the probability of dying.

Dallek & Foley [7] investigated the influence of anions on the initiation of pitting and kinetics of pit

growth on aluminum alloy type 7075. The rate equation is then

$$(1/\tau) = k\ [Al]^m\ [X^-]^n. \qquad (12)$$

where $(1/\tau)$, the reciprocal of the induction time, is taken as the rate of pit initiation,

k is the rate constant,

[Al] the aluminum atom concentration,

$[X^-]$ the halide ion concentration, and

m and n are the respective orders of reaction.

A deterministic treatment for the pitting of Fe-17Cr is presented by Macdonald [8], for the statistical nature of the breakdown treatment of films on metal surfaces in which it is assumed that breakdown sites on the surface are distributed normally in terms of the cation vacancy diffusivity. This analysis, which is based on the point defect model for the breakdown of passive films, predicts a near-normal distribution in the breakdown voltage, but a high asymmetric distribution in the induction time. The model is able to account for the experimental observed distribution in the breakdown voltage and induction time for the pitting of Fe-17Cr in 3.5% NaCl solution at 30 °C, as reported by T. Shibata (1983) and T. Shibata and T. Takeyama (1976-1981).

3. TESTING PROBLEMS

The American Society of Testing and Materials Committee G-1 have generated several series of field tests for a variety of materials at five locations since 1907. Tests have triplicate exposed panels for removal periods of 1, 2, 3, 5, 7, 10, 20 years. Evaluation of these materials includes weight losses, pitting depth, and changes in mechanical properties. Results have been reported widely, [4], [10], [11], [12], [13], [14] as averages. These data will be discussed later.

The purposes of these tests, among other, was to estimate corrosion resistance for different metallic systems and their protection (including commercial products) under different working and storage conditions. Even though only three or five samples of each material were removed at various time intervals, the total number of panels was still large.

The dispersion of result also was large, Table 2, often several times the mean value. Commonly, one specimen had corroded severely, while an adjacent identical specimen was uncorroded. Considering this dispersion, the life prediction only can be made within a probability limit as in the case of fatigue. Figure 4 shows the schematic diagram of fatigue P-S-N curve.

If a corrosion initiation time distribution can be determined and combined with suitable kinetics and

Table 2 Larrabee-coburn Data from Kearny, N.J., Compared with that from South Bend, PA.

Data Factor	Kearny, New Jersey	South Bend, Pennsylvania
No. of observations	270	270
Mean corrosion rate(mils)	4.500	4.164
Standard deviation	3.732	1.989
Highest observation	41.7	16.5
Lowest observation	1.6	1.3
Range	40.1	15.2

from "The Statistic Analysis of Atmospheric Corrosion Data"
by R. A. Legault & J. G. Dalal

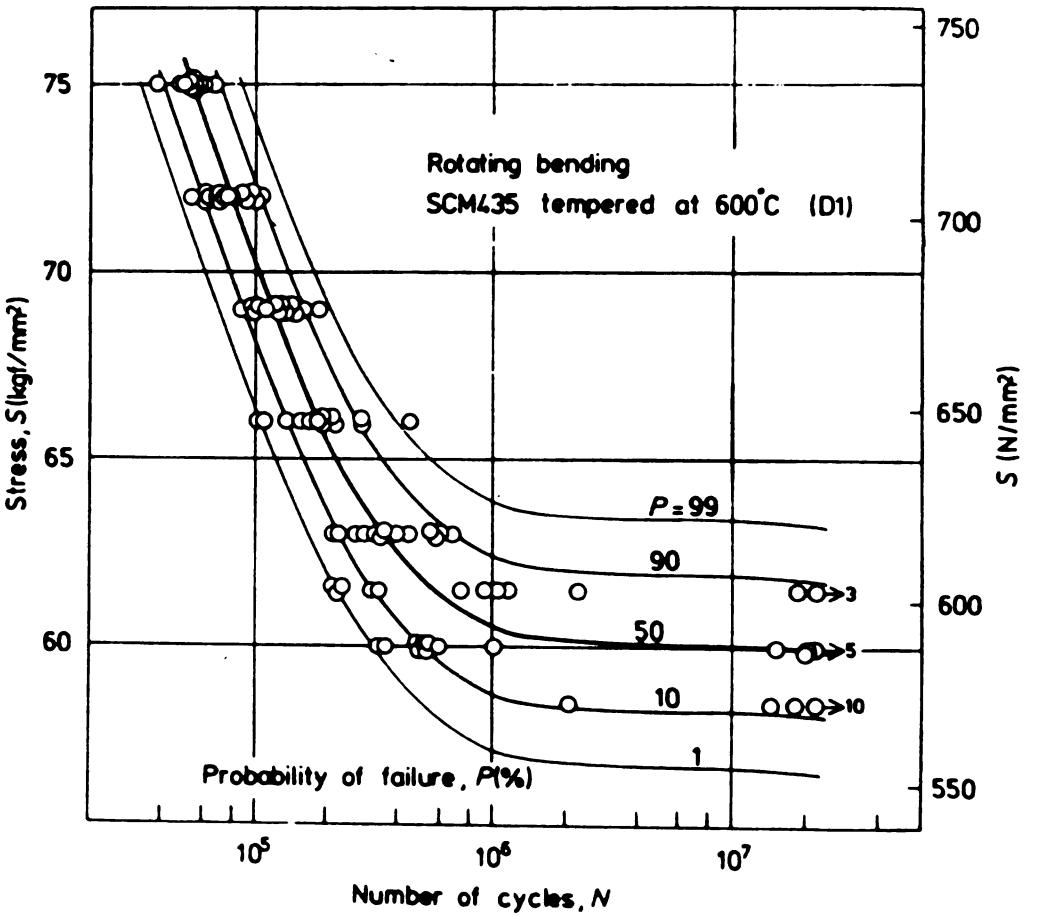

Figure 4. Fatigue probability-stress-cycles, P-S-N, diagram.

statistical treatment, a predicted damage level at certain exposure time or failure life can be computed.

III EXPERIMENTAL

1. EXPERIMENT DESIGN

Suppose that the observed variance in corrosion test data results largely from dispersion of a stochastic initiation process and random sampling followed by uniform corrosion kinetics, which would be the same for specimens of the same materials in a uniform corrosive environment. Then it would follow that at any time after initial exposure, these specimens would exhibit different amounts of corrosion damage in some proportion to their different time of initiation. In a real environment, of course, the corrosivity might change and such changes would accentuate or diminish differences caused by the initiation rate. For example, environmental severity may worsen between the time of initiation of sample i and sample j, thus the difference between the two samples at a time following the initiation of i would be larger than otherwise expected. Likewise, if the conditions became milder, the difference would be narrowed. There appear to be no published efforts to determine such initiation distributions experimentally, although some stochastic models have been suggested. The difficulties are that the corrosion initiation is hard to detect and evaluate, and a large number of specimens are

needed.

We have designed deliberately simple-minded experiments with a simple criterion to detect initiation. Since true initiation occurs on a microscopic scale, it is not detectable, consequently, first visible observation of corrosion was used as the criterion, assuming that the short time interval between initiation and observation does not distort the results significantly. This is not unlike the use of 0.02% offset in tensile testing to determine the yield stress of a metal.

Immersion of zinc coupons into aqueous 1.0 N hydrochloric acid would result in near-instantaneous initiation in all samples, hence the initiation times could not be measured. At the other extreme, atmospheric exposure of aluminum in desert conditions would exhibit corrosion initiations spread over several years.

All specimens should be placed simultaneously in the same environment with the corrosivity held constant. Using a statistically valid number of specimens, these tests should provide sufficient data for analysis.

The purpose of the experiments is to construct a model for corrosion initiation, two systems were selected: plain-carbon steel in a humid atmosphere and an aluminum alloy immersed in aqueous sodium chloride. These environments were selected to be severe so that initiation would occur over a short time period.

2. PROCEDURE

Experiment I was performed in a Blue M Electric Vapor-Temp Cnamber Model VP-100, Figure 5, with controlled humidity and temperature.

The 25 plain-carbon steel carpenters nails were cleaned by conventional procedures, i.e. with 600# grit abrasive paper removal of rust, and rinsing with acetone and petroleum ether to remove oils. Following cleaning, no rust or stain was visible at 100x magnification.

The samples were hung from a rack in the chamber with nynon filament and at

relative humidity: 90±5%

temperature: 85 ±5°F.

The above conditions were calibrated before testing.
The initiation time of individual smples was recorded when the first visible orange stain appeared on the surface.

Experiment II used immersion of AA 2024-T3 in 0.01N aqueous NaCl without stirring. The specimens were cut into 3/4" x 1 1/2" x 1/16" coupons, with a hole near the top for hanging on glass hooks. The samples were wet polished with 400# grit and 600# grit abrasive paper, rinsed, and degreased with acetone. No evidence of corrosion was visible at 400x magnification, see Figure 6. The second

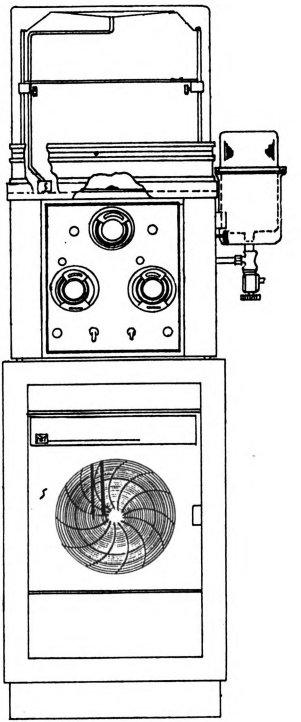

Figure 5. Blue M Electric Vapor-Temp Humidity Chamber

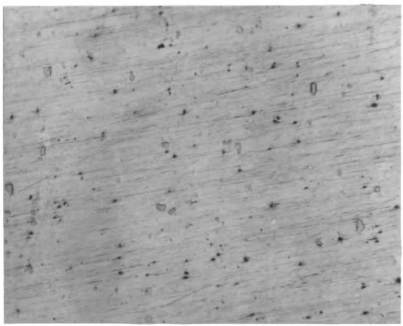

400x

Figure 6. AA 2024-T3 coupon surface before immersion

phase particles or impurities appear grey or white surrounded by phase boundaries. Following cleaning, the samples were allowed to stand for at least 24 hours in a desiccator.

The 100 specimens were mounted with glass hooks, immersed in 0.01 N NaCl (PH = 7.0) at room temperature (70° F) and removed when the first stain appeared. The beginning and end times were recorded for each sample. The samples were cleaned with distilled water to wash the precipitates off, and then dried.

After that, the samples were examined carefully under the microscope, to be sure that the determination of initiation time was made at the same damage level. The second phase particles appeared dark and were surrounded by a coloured halo.

Figure 7 shows the different corrosion results of these samples immersed in 0.01 N NaCl for same time 220 minutes:

(a) corrosion initiated

(b) corrosion coloured halo appeared

(c) corrosion developed

The criterion was set at Figure 7 (b).

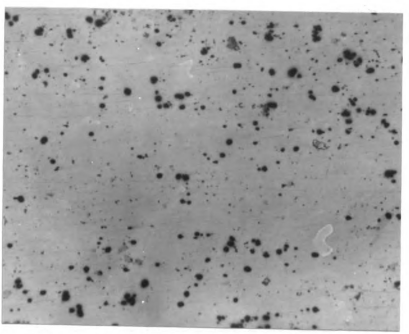

400x

(a)

Figure 7. AA 2024-T3 coupon surface after 220 minutes immersion.

(a) corrosion initiated

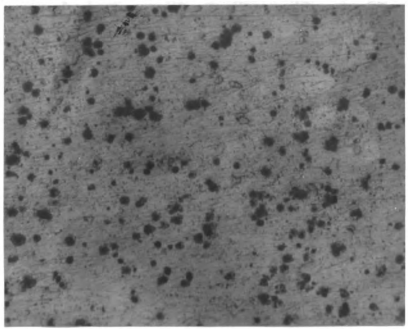

400x

(b)

Figure 7. AA 2024-T3 coupon surface after 220 minutes immersion.

(b) corrosion coloured halo appeared

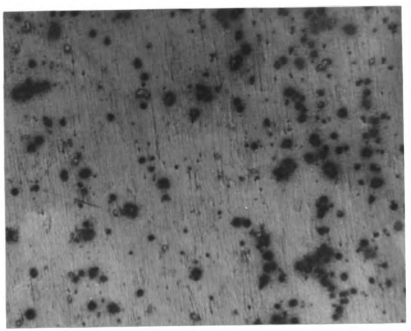

400x

(c)

Figure 7. AA 2024-T3 coupon surface after 220 minutes immersion.

(c) corrosion developed

IV. RESULTS

1. DATA

Plain carbon steel nails:

Table 3 Corrosion Initiation Time For Nails

Initiation Time (hours)				
2.2	2.9	3.3	3.7	3.9
4.3	4.5	4.8	5.1	5.4
5.8	6.2	6.6	7.1	7.6
8.1	8.7	9.5	10.1	10.8
1.8	12.8	13.9	15.7	20.0

$$\text{sample mean} = \frac{1}{n}\sum_{1}^{25} X_i = 7.7918$$

$$\text{sample variance} = \frac{1}{n}\sum_{1}^{25} (X_i - \bar{X})^2 = 18.7556$$

$$\text{standard deviation} = 4.33$$

AA 2024-T3 coupon salt immertion

Table 4 Corrosion Initiation Time For AA 2024-T3 coupons

Initiation Time (minutes)				
218	222	223	225	226
227	228	229	230	231
231	232	233	233	234
234	235	236	236	237
237	237	238	238	239
239	239	240	241	242
242	243	243	243	243
244	244	244	245	245
246	246	246	246	247
247	247	248	249	249
250	250	250	251	251
252	253	253	253	254
254	256	257	258	258
259	259	260	261	262
263	263	264	264	266
267	267	269	269	270
271	272	274	274	277
277	278	278	279	280
281	282	283	285	287
289	291	292	293	307

$$\text{sample mean} = \frac{1}{n}\sum_{i}^{100} X_i = 253.13$$

$$\text{sample variance} = \frac{1}{n}\sum_{i}^{100} (X_i-\bar{X})^2 = 356.17$$

$$\text{third moment} = \frac{1}{n}\sum_{i}^{100} (X_i-\bar{X})^3 = 3646.55$$

standard deviation = 18.87

2. STATISTICAL ANALYSIS

An empirical distribution function (edf) of corrosion initiation time data for nails is shown in Figure 8. The abscissa is time measured in hours, and the ordinate is fraction initiated. The estimated mean and variance are 7.79 and 18.76, respectively. Curve 2, a cumulative distribution function of Gamma distribution based on the above mean and variance accurately describing this edf, incorporates these features in a quantitative manner. The signal-to-noise ratio, m /σ is 1.80.

An empirical distribution function (edf) of corrosion initiation time data for AA 2024-T3 coupons in salt immersion is shown in Figure 9. The abscissa is time measured in minutes, and the ordinate is fraction initiated. The estimated mean and variance are 253.1 and 356.1, respectively. The signal-to-noise ratio, m / σ is 13.41. Curve 2, generated cdf of Gamma distribution based on the above mean and variance, incorporates the edf very well.

Figure 10 shows the histogram of corrosion initiation time for nails. The abscissa is time t measured in hours and the ordinate is frequency, indicates during the time

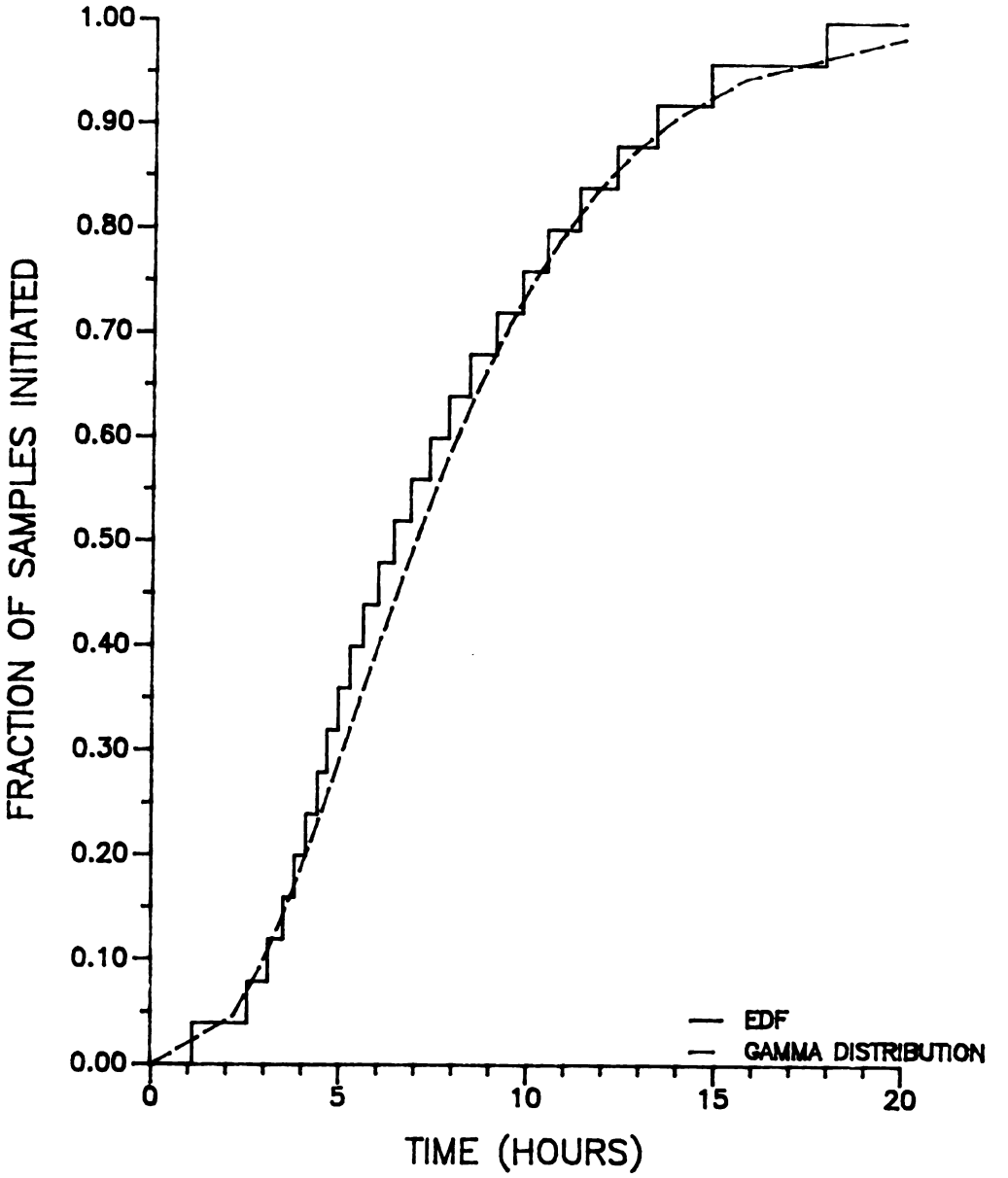

FIGURE 8. AN EDF OF INITIATION CORROSION TIME DATA FOR NAILS

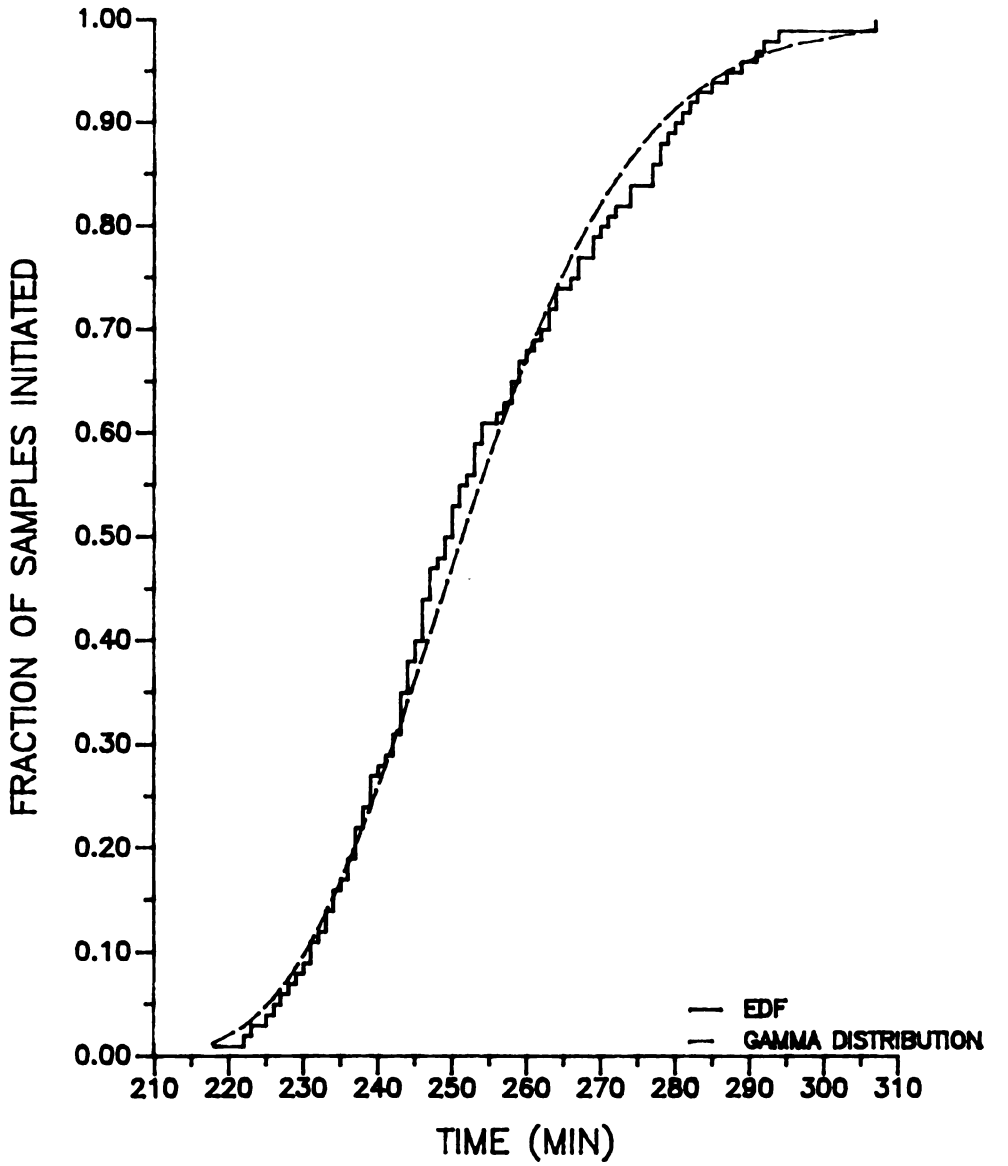

FIGURE 9. AN EDF OF INITIATION CORROSION TIME DATA FOR AA 2024–T3 COUPON

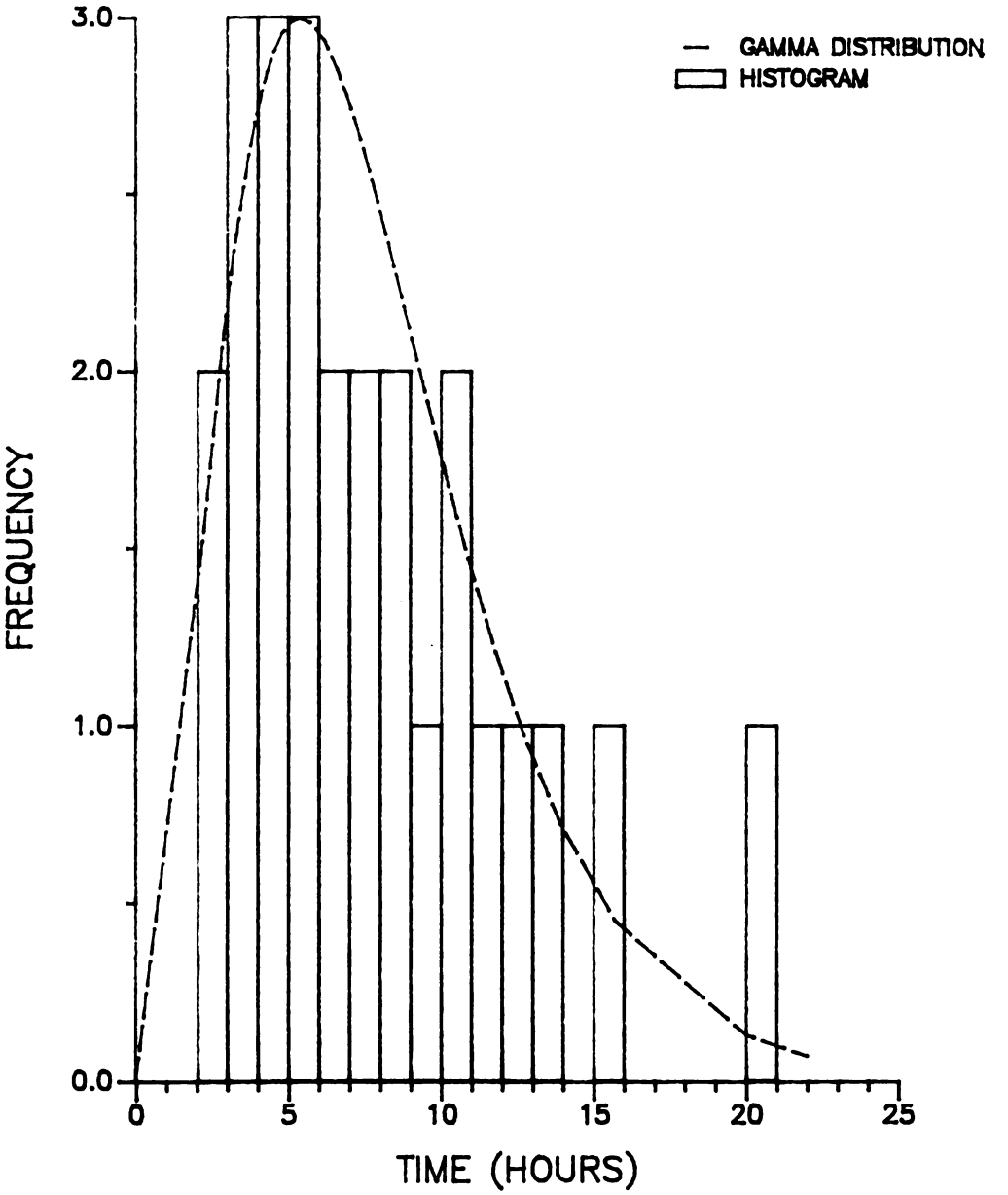

FIGURE 10. HISTOGRAM OF INITIATION TIME DATA FOR NAILS

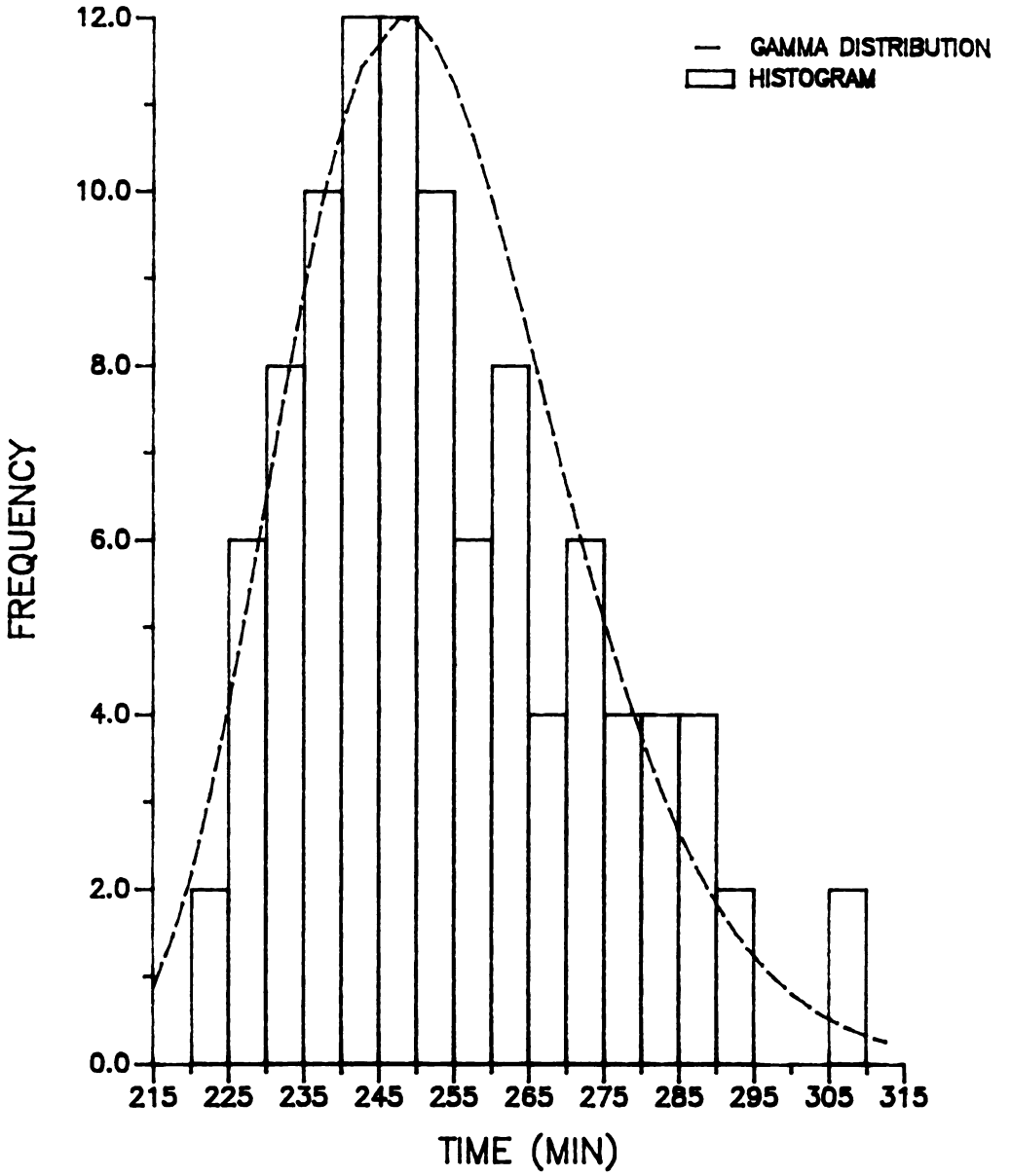

FIGURE 11. HISTOGRAM OF INITIATION TIME DATA FOR AA 2024–T3 COUPON

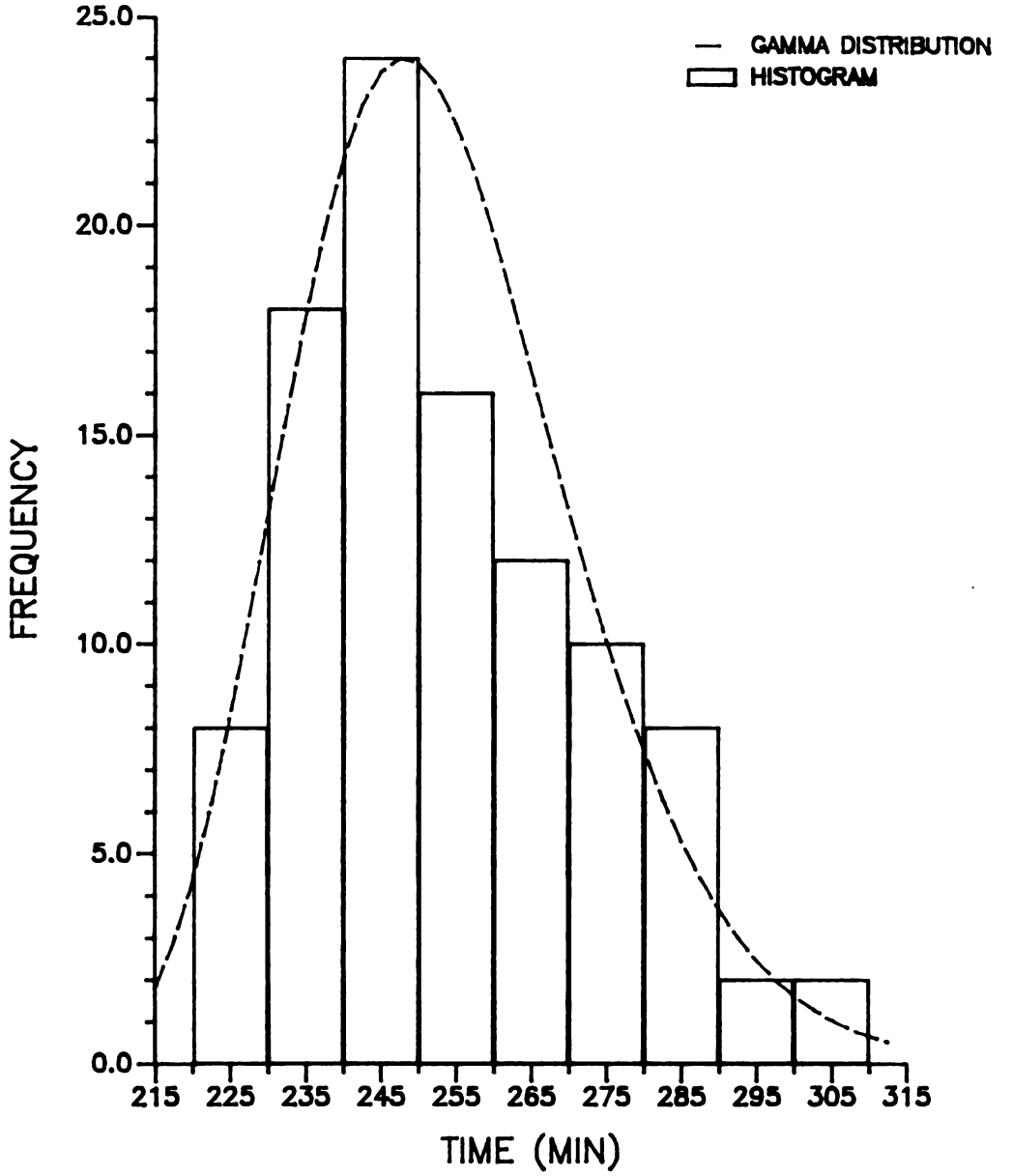

FIGURE 12. HISTOGRAM OF INITIATION TIME DATA FOR AA 2024–T3 COUPON

interval, 1 hour, how many nails exhibited corrosion initiation. The Gamma distribution function (pdf) added on this histogram, fitted the histogram.

Figures 11 and 12 show the histograms of initiation time for AA 2024-T3 coupons salt immersion, the frequencies in different time interval 5 minutes and 10 minutes. A pdf of Gamma distribution function attached on the histogram, which fitted the histogram well.

A test of the null hypothesis shows that the initiation time distribution follows a Gamma distribution function for nails and AA 2024-T3 coupons, respectively, hence hypothesis test cannot be rejected. Hence, the corrosion initiation time distribution model is:

$$f(\sigma;\ \theta,R,\alpha) = \frac{1}{\Gamma(R)\theta^{R}}\ (\sigma-\alpha)^{R-1}\exp[-\frac{\sigma-\alpha}{\theta}], \qquad (13)$$

where $f(\tau;\ \theta,r,\alpha)$, the probability density function, indicates the corresponding probability of initiation time τ,

τ is the initiation time of corrosion different from the exposure time,

θ, R, α are parameters, depending on the individual materials, environments and geometry.

In the case of nails:

R = 3.237,

θ = 2.4071,

α = 0

In the case of AA 2024-T3 coupon salt immersion:

R = 13.5918,

θ = 5.1191,

α = 183.55.

V DISCUSSION

1. INITIATION TIME MODEL

It is presented by some authors, Summitt [5], et al. theoretically that the corrosion initiation process, like most cumulative damage processes, fulfills the stochastic process-- Poisson process. Let us start at this point, i.e. the specimen can only be corroded or not corroded at any point in time, which might be a specific discrete state.

Let N(t) denote the number of samples corroded in (0,t]

$P_k = P\{ N(t) = k \}$ $\quad k = 0, 1, 2, \ldots$

thus P_k (t) is the probability that k specimens have corroded in the time interval (0,t]. Then the random variable $N(t+\Delta t) - N(t)$ is the number of specimens corroded in the interval Δt.

Suppose the N(t), $N(t+\Delta t)-N(t)$ have same distribution and are independent of what happens at or before t.

$$P\{ N(\Delta t) = 0 \} = P_0(\Delta t) = 1 - \lambda\Delta t + o(\Delta t)$$

$$P\{ N(t+\Delta t - N(t) = 0 \} = P\{ N(t) = 0 \}$$

$$= 1 - \lambda\Delta t + o(\Delta t)$$

$$P_0(t+\Delta t) = P\{ N(t+\Delta t) = 0 \}$$

$$= P\{ N(t) = 0, N(t+\Delta t) - N(t) = 0 \}$$

$$= P \{ N(t) = 0 \} P \{N(t+_T t) - N(t) = 0 \}$$

$$= P_0(t) \{ 1 - \lambda\Delta t + o(\Delta t) \}$$

where it is assumed that each specimen corroded independently or

$$P_0'(t) = - \lambda P_0(t).$$

Solve the differential equation,

$$P_0(t) = e^{-\lambda t} \qquad t \geq 0.$$

Continuing in this manner, we find that

$$P_k = \frac{(\lambda t)^k}{k!} e^{-\lambda t} \qquad k = 0, 1, \ldots \qquad t \geq 0. \qquad (14)$$

We see that at any time t, N(t) the number of specimens corroded has the Poisson distribution with parameter λt. Figure 13 shows the $P_j(t)$ as a function of j and t. We obtain from Equation (14)

$$P \{ N(t) = 0 \} = e^{-\lambda t}$$

Let the random variable T denote the time from 0 to the first corroded (initiation time). Then

$$P \{ T > t \} = P \{ N(t) = 0 \} = e^{-\lambda t}.$$

$$F_T(t) = P \{ T \geq t \} = 1 - P \{ T > t \} = 1 - e^{-\lambda t}.$$

Let τ_k denote the time to the kth corrosion. It follows that

$$\tau_k = T_1 + T_2 + T_3 + \ldots + T_k \qquad k = 1, 2, \ldots \qquad (15)$$

T_k denote the time from $(k-1)^{th}$ specimens corroded to the kth

τ_k and N(t) are related through their distributions:

$N(t) \geq k$ means k or less corrosions have taken place in $(0, t]$

So $$F_N(k;t) = 1 - F_\tau(t; k+1) \qquad (16)$$

Since $$F_N(k;t) = \sum_0^k e^{-\lambda t} \frac{(\lambda t)^j}{j!}.$$

We obtain the pdf of τ_{k+1} is

$$f_\tau(t; k+1) = \frac{\lambda(\lambda t)^k e^{-\lambda t}}{k!} \qquad t>0$$
$$= 0 \qquad \text{elsewhere} \qquad (17)$$

Let $\lambda = \frac{1}{\theta}$ $\quad R = k+1$ $\quad t = \tau - \alpha$

$$f_\tau(\tau - \alpha; R) = \frac{1}{(R-1)!\theta^R} (\tau-\alpha)^{R-1} \exp[-\frac{\tau-\alpha}{\theta}]$$

$$= \frac{1}{\Gamma(R)\theta^R} (\tau-\alpha)^{R-1} \exp[-\frac{\tau-\alpha}{\theta}] \qquad (18)$$

Equation (14) is as the same as the pdf (probability density function) of Gamma distribution drawn from the experimental data (9).

So far, from the experimental hypothesis tests of the corrosion initiation time or from the analysis of the stochastic process, we get the same function. All confirm

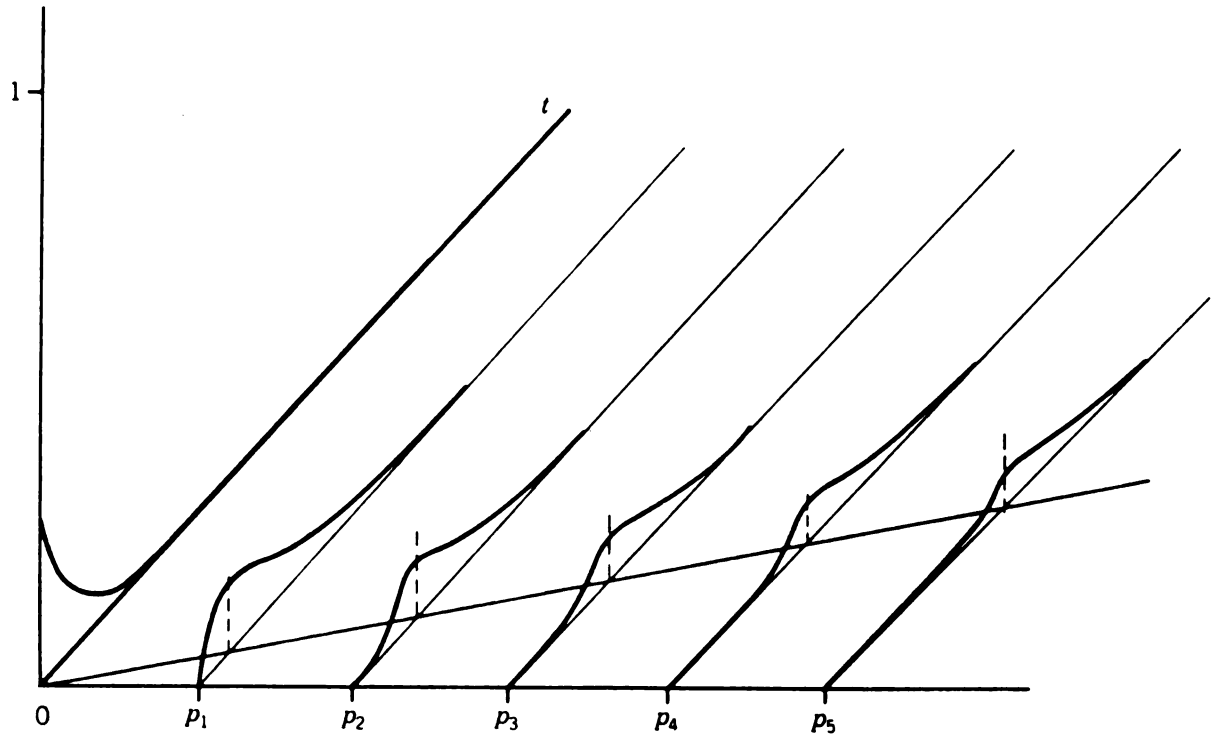

Figure 13. Evalution of P_j (t) with time for Poisson process.

that the corrosion initiation time distribution model is a Gamma distribution, which has physical meaning, and fitted the experimental data very well.

Further, by the central limit theorem, as $R \to \infty$, the r are asymptotically normally distributed.

2. PROJECTION TO "LONG TIME" DAMAGE DISTRIBUTION

Like fatigue, one can build a P-D-T diagram to predict corrosion damage. The Probability-Damage-Exposure time diagram, a family of D-T curves each corresponding to a particular value of probability, can adequately express the two concepts of scatter, i.e., damage scatter-distribution, (P-D) and life (exposure time) scatter-distribution (P-T). An ordinary way of establishing such a P-D-T diagram for a given material in a given environment is to determine experimentally the P-T relations at different corrosion damage values and draw a P-D curve using t values expected for the P prescibed. Obviously, a hundred tests are needed to get t values at P = 1 percent for only a single value of D. It is not ratical to run hundreds of corrosion field tests.

The aim of this paper is to project corrosion. So we attempt to give a more practical method of producing P-D-T diagrams with an accessible number of specimens. From the

previous discussion, it is obvious that the exposure time should be divided by two periods: one for corrosion initiation, one for corrosion development, so that the kinetical equation should be modified as follows:

$$W = A (t - \tau)^{b} \qquad (19)$$

where t is the total exposure time

τ is the initiation time, depending on probability prescribed,

$t - \tau$ is the actual corrosion reaction time, and

A, b parameters, depend on the materials and environment.

One can use this formula and corrosion initiation distribution model to predict long time damage distribution.

Theoretically, for each damage level, there is an exposure time distribution function with its own parameters, simular to the initiation time distribution-Gamma function respectively. The individual D-T curve might be made by calculating the exposure time corresponding to a given probability, shown in Figure 15. Figure 14 and equation (20) illustrate the method to decide the exposure time, i.e.

Probability that corroded within time interval (o,t]

= the area under the curve until t_{τ}.

The more convenient way is to calculate the initiation time corresponding to the given probability and shift the

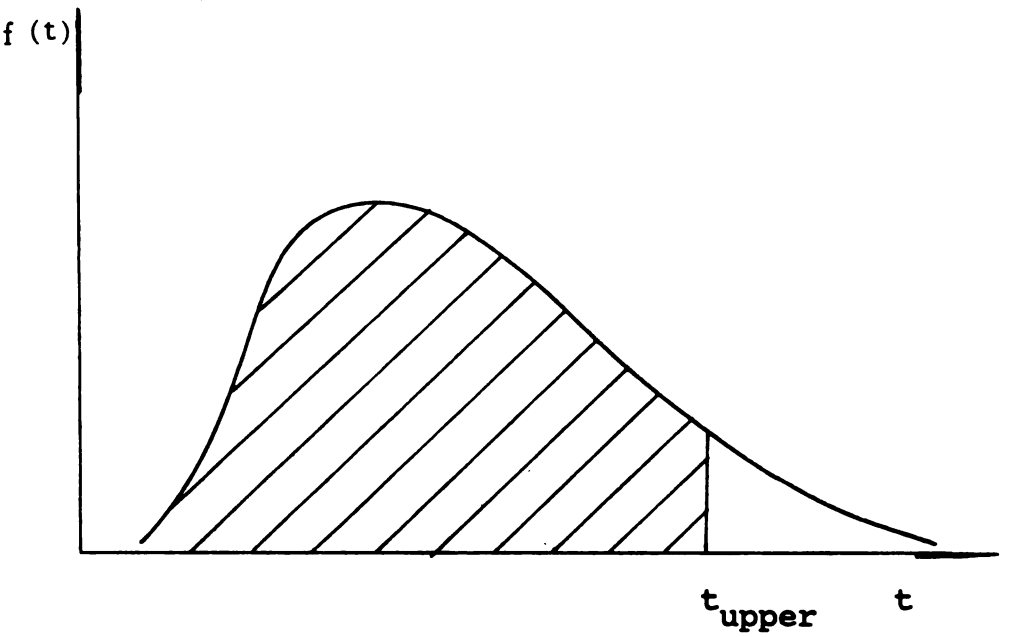

$$\text{PROB}\,[\,T < t_{upper}\,] = \text{AREA}$$

$$= \int_0^{t_{upper}} f\,(t)\,dt$$

$$= \int_0^{t_{upper}} \frac{1}{\Gamma(R)\,\theta^R}\,(\,t - \alpha\,)^{R-1} \exp\left[-\frac{t-\alpha}{\theta}\right] dt$$

$$= \gamma \qquad (20)$$

Figure 14. In illustration of probability-time curve

D-T curve along the time axis for calculated initiation time, as in Figure 15. Here, assume that the sample which initiates early corresponds to larger damage. In this way, one can get the damage band for a specific material and predict the damage which exist at any arbitrary exposure time with some confidence.

Meanwhile, one can recognize that the distribution is a two-way distribution shown schematically in Figure 15, i.e. in exposure time and in damage. The shape of the exposure time distribution is strongly dependent on the damage level, but the damage distribution appears to show similarities at different exposure time. Since the Gamma distributions are skewed negatively as shown, the scatter will tend to high value. This phenominon is expected to explain the large dispersion of the data.

As a test of Equation (15), several sets of data for low alloy steels were selected from the literature [10]. Their chemical compositions are shown in Table 5, weight losses in Table 6, and the compared experimental and calculated weight losses in Table 7.

From Table 7, the calculated values are generally underestimated, although the predicted and actual values are very close. This assumption shows that the rate law $W = A(t - \tau)^b$ is valid as far as deviation less than ±10%. In addition, the above actual values are the average of two or four experimental data points, so the predicted values

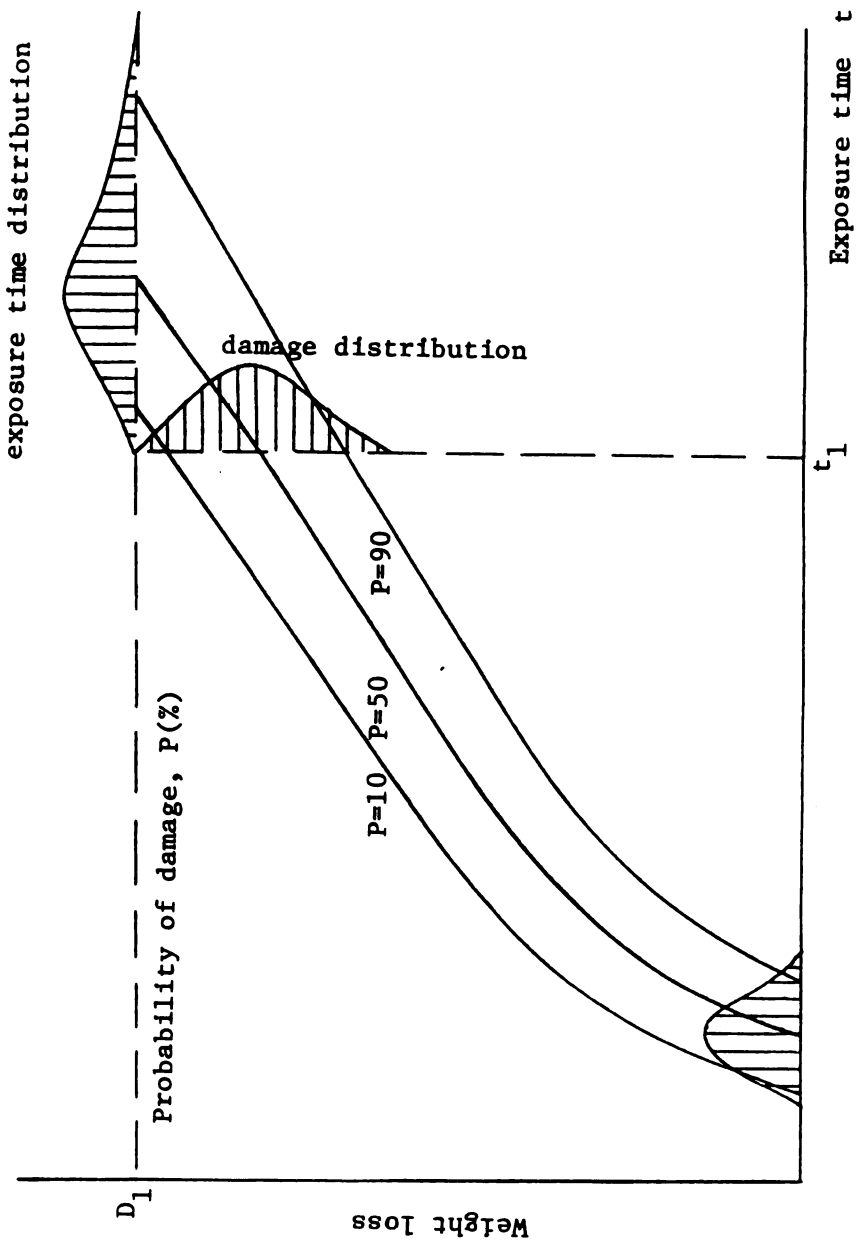

Figure 15. Two-way distributions shown schematic P-T and P-D relationships

Table 5. Analysis of Steel

Steel	Analysis per cent								
	C	Mn	Si	S	P	Ni	Cu	Cr	Mo
No.48	0.17	0.89	0.05	0.03	0.075	0.16	0.47	--	0.28
No.63	0.02	0.023	0.002	0.03	0.005	0.05	0.053	--	--
No.10	0.041	0.22	0.002	0.04	0.01	0.05	0.02	0.01	--
No.13	0.072	0.27	0.83	0.02	0.14	0.03	0.46	1.19	--
No.32	0.11	0.69	0.14	0.02	0.011	0.20	0.038	--	--
No.54	0.02	0.07	0.01	0.03	0.003	0.18	0.10	--	--
No.11	0.04	0.49	0.003	0.04	0.074	0.01	0.05	0.10	0.003

Table 6. Weight Loss, g dm^{-2}.

Steel	Kure Beach N. C.					Bayonne, N. J.				
	years of exposure									
	0.5	1.5	3.5	7.5	15.5	1.0	3.0	5.1	7.1	9.1
No.32	2.1	3.9	7.4	13.1	21.5	4.7	7.2	8.8	10.5	12.2
No.54	2.5	4.8	8.9	15.0	26.5	5.1	8.3	10.3	12.8	13.5
No.11	2.1	4.2	8.1	13.5	20.9	4.9	7.9	9.7	12.0	12.6
No.48	1.8	3.5	4.9	7.9	11.8	3.0	--	5.1	--	6.5
No.63	2.3	4.8	10.1	19.0	43.0	5.8	10.1	11.3	--	16.1
No.13	1.6	3.5	4.9	7.9	11.8	1.8	--	2.6	3.2	3.5
No.10	2.6	5.0	10.3	19.7	--	5.6	9.3	11.3	14.5	17.7

Table 7. Experimental and Calculated Weight Losses for Two Sites

Steel	Kure Beach (15.5 yr)			Bayonne (9.1 yr)		
	Experimental	Calculated	Experiment / Calculated	Experimental	Calculated	Experiment / Calculated
No.32	21.5	20.86	1.03	12.2	11.44	1.066
No.54	26.5	25.39	1.043	13.5	13.13	1.028
No.11	20.9	21.06	0.992	12.6	12.374	1.018

are for 50 % confidence (not actually for the average values are suspensive as population mean in so small sample space). Considering the number of the samples and experimental error, this result is good.

Most literature data are reported as means and standard deviations, hence no original data were available for doing a thorough statistical treatment.

3. EXTENSION TO A LESS SEVERE ENVIRONMENT

Corrosion process is a complex process, which can be affected by many factors, e.g., water SO_2, chloride etc., and synergistic effects are possible. The overall process can be separated into several subprocesses, each with its own transition probability function. When the environment and materials are set, the probability space is set by a stochastic matrix at certain time,

$$P = \begin{bmatrix} P_{11}(t,s), & P_{12}(t,s), \ldots, & P_{1n}(t,s) \\ \vdots & \vdots & \vdots \\ P_{n1}(t,s), & P_{n2}(t,s), \ldots, & P_{nn}(t,s) \end{bmatrix}$$

P_{ij} represents the one step transition probability from state i to state j,

s, are various factors which influence the probability, e.g., temperature

In a Markoff process, each P_{ij} depends only on the state i-1, and is independent of other states.

So from initiation state to final state, the probability $P\{E_{j_k}\}$ at the kth step is

$$P\{E_{j_k}\} = \sum \cdots \sum a_{j_0} P_{j_0 j_1} \cdots P_{j_{k-1} j_k} ,$$

Using matrix notation

$$P_k = P_0 \quad P^k . \tag{17}$$

Different combinations of environment and material have a different probability matrix, for example, if the environment includes Cl^-, $SO_4^=$, and moisture, the matrix will be more complicated, and the corrosivity more severe.

For such a Markoff process, if time is a continuous variable, this stochastic process is still a Poisson process with the time distribution corresponding to Gamma, but the parameters are changed, depending on the materials and environments.

Analyses of the data from ASTM tests, Tables 6,7,8, were made for comparisons on the basis of environment and of materials. At Kure Beach, N.C. a marine site 240 m from the ocean, the main corrosive factor is Cl^-. Bayonne, N.J. is an industrial location not far from a center of oil refining activity.

Comparing the parameters of two groups, Table 8, a noticeable feature is that all the initiation times of three steels at Bayonne decreased, the exponent b decreased approximately 3/5 of those in Kure Beach, but A for steels

at Bayonne increased as 1 1/3 times those in Kure Beach. This feature is fitted to the steel corrosion mechanism that, during the very early stages of exposure, the weight loss depends on the environment, and later depends on the water which can reach the surface through the corrosion products. In Bayonne, the main pollutant is sulfur dioxide, so the steel corroded very fast; at Kure Beach, the main environmental factor is chloride., its high solubility would be expected to make it more difficult to plug pores in the rust coating. Corrosion rates have been decreasing more slowly at Kure Beach than Bayonne, as shown in Figures 16, 17, 18.

From the above examples, one suggestion might be made that all parameters are functions of corrosivity factors or proper coefficients. In turn, however, one can predict the damage to a material in an untested environment. Of course, it is obvious that the kinetic equation cannot be extrapolated to an other environment using only P_1, P_2 damage coefficients from the literature [1].

Comparing the calculated parameters of two groups of steels at Kure Beach, it is found that changing some alloy elements will change the values of parameters considerably. No.48 steel has more manganese (0.87%) and copper (0.42%) than No.63, and its A value decreases 0.8 and the exponential b 0.323. No.13 steel has more silicon (0.83%), copper (0.44%) and chromium (1.128%) than No.10, and its A

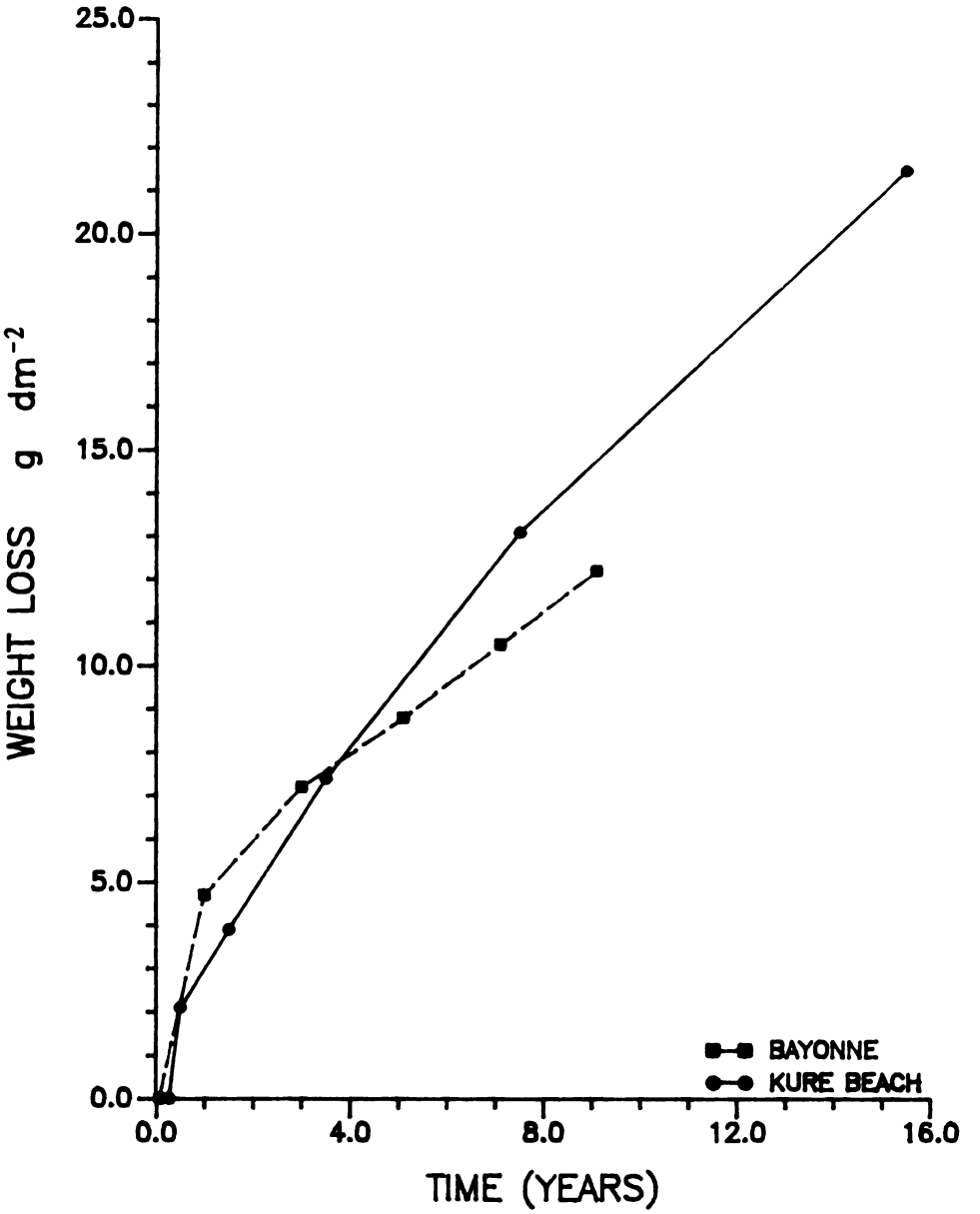

FIGURE 16. WEIGHT LOSS–TIME CURVE FOR NO.32 STEEL AT KURE BEACH & BAYONNE

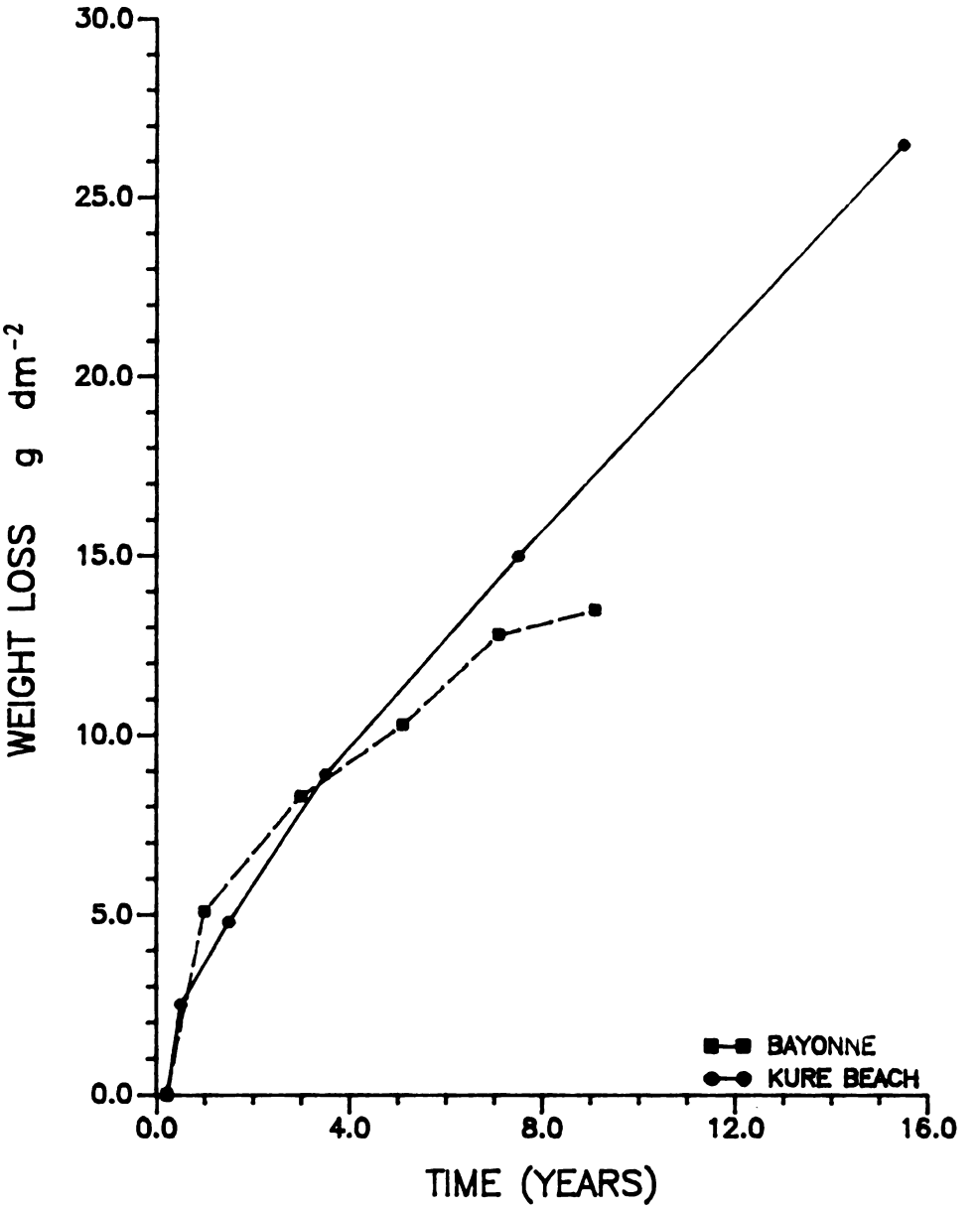

FIGURE 17. WEIGHT LOSS–TIME CURVE FOR NO.54 STEEL AT KURE BEACH & BAYONNE

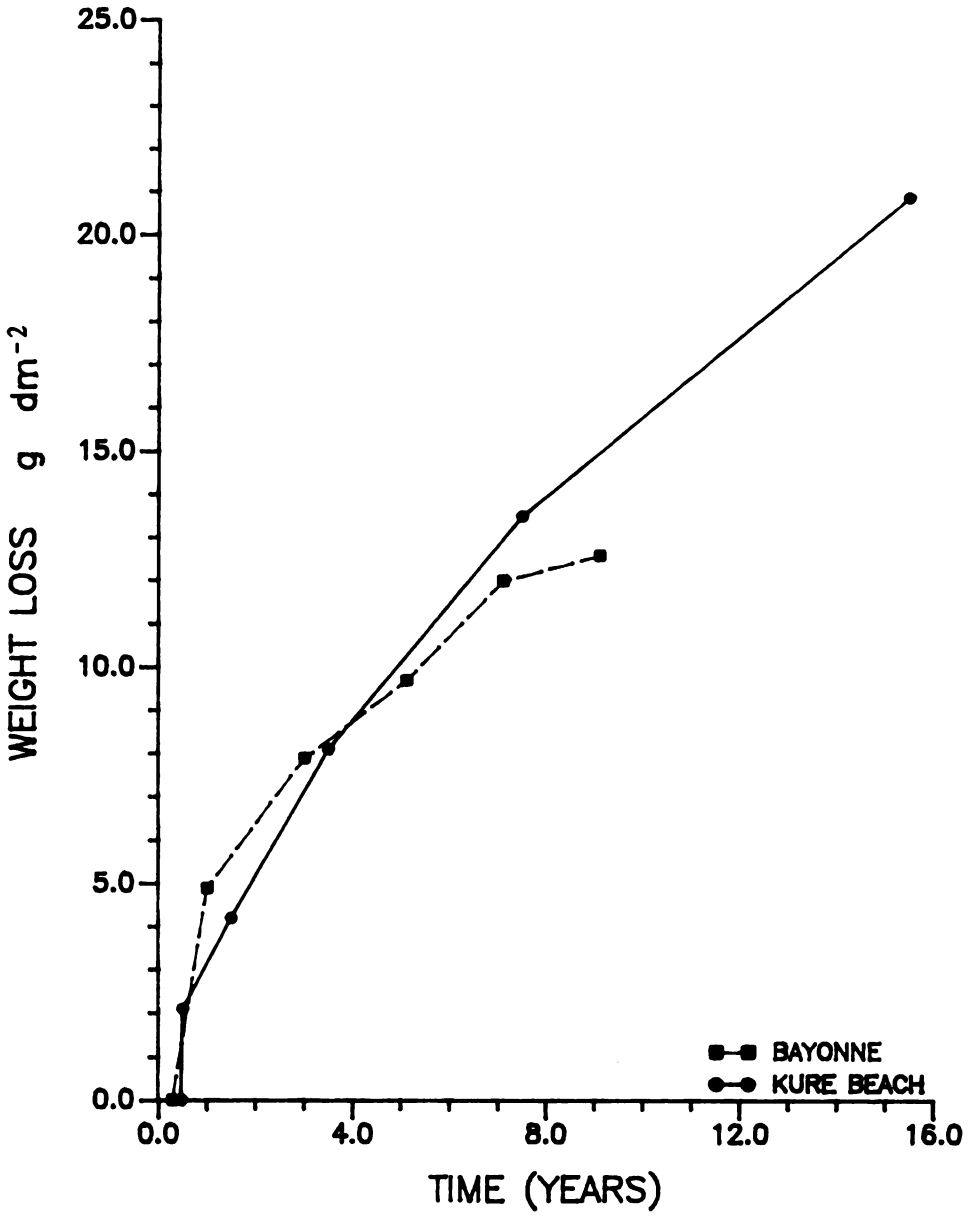

FIGURE 18. WEIGHT LOSS–TIME CURVE FOR NO.11 STEEL AT KURE BEACH & BAYONNE

Table 8. Calculated Parameters at Kure Beach & Bayonne

Steel	parameters	Kure Beach	Bayonne
No.32	A	3.44	4.85
	b	0.666	0.39
	r	0.264	0.072
No.54	A	4.2	5.61
	b	0.66	0.39
	r	0.2275	0.217
No.11	A	4.145	5.53
	b	0.6	0.37
	r	0.478	0.283

Table 9. Calculated Parameters of Four Steels at Kure Beach

Steel	A	b	r
No.48	3.055	0.477	0.17
No.63	3.866	0.8	0.182
No.10	3.564	0.849	0.01
No.13	2.196	0.389	0.098

value decreases 1.37, b value decreases 0.46; the decreasing in b is significant, only as half as those of No.10. So corrodibility of the material also should be considered.

In extending to a less severe environment, one formula might be suggested:

$$W = A(s,m)\,[\,t - \tau(s,m)\,]^{b(s,m)}, \qquad (18)$$

where s is a corrosivity factor depending on environments,

m is a material factor depending on corrodibility of the materials, and

$\tau(m,s)$ mainly depends on environment through the initiation time function parameters α, R, θ.

Since no actual experimental data are available in the literature, it is not possible to check further the agreement between our formula and experimental results. Further long term exposure tests will be performed to produce data.

It is possible apparantly to predict damage in a less severe environment using the above model. It is too early to draw general conclusions from these tests of limited nature. Further investigation will produce original data to find the relationship.

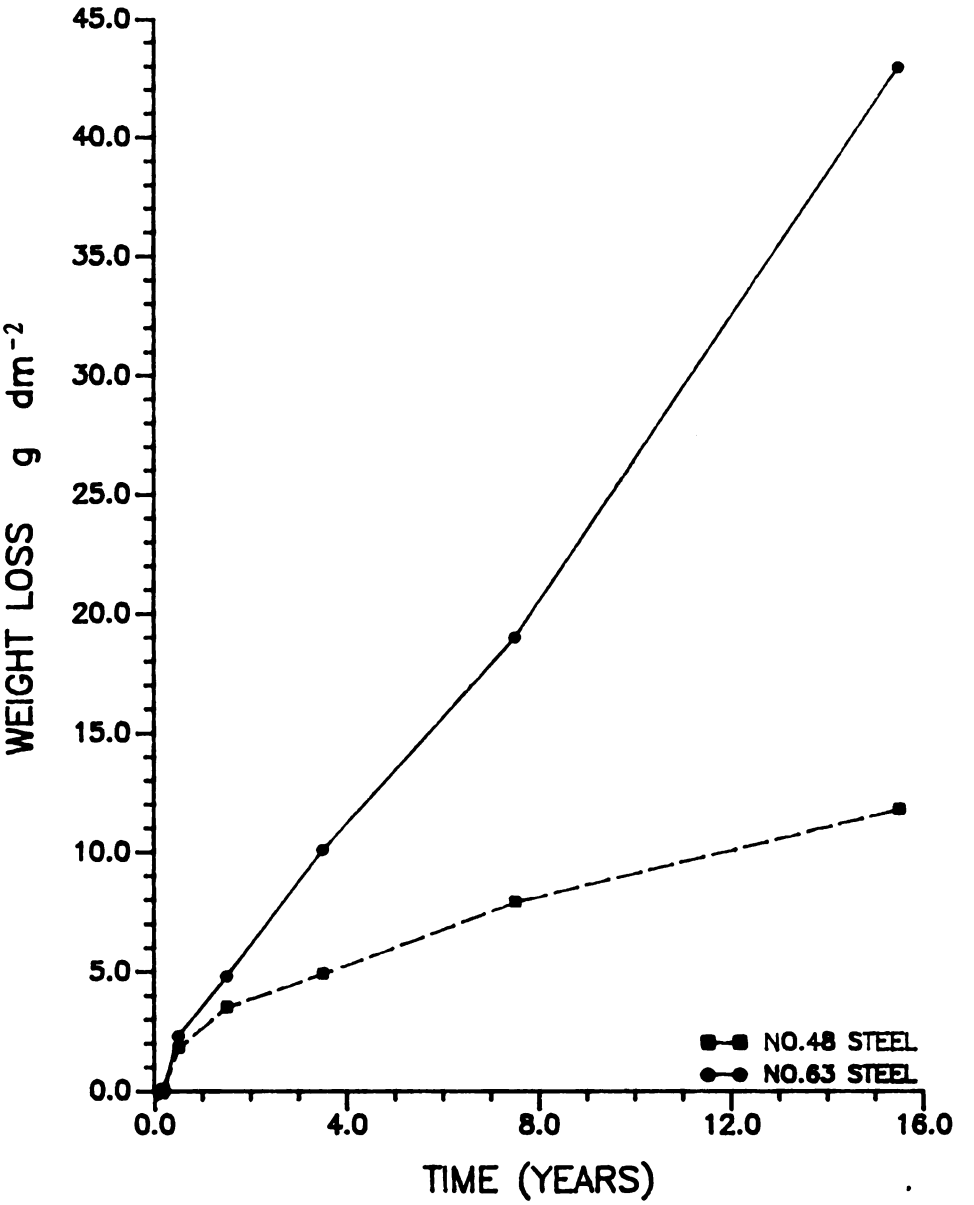

FIGURE 19. WEIGHT LOSS–TIME CURVE FOR NO.63 & NO.48 STEELS AT KURE BEACH

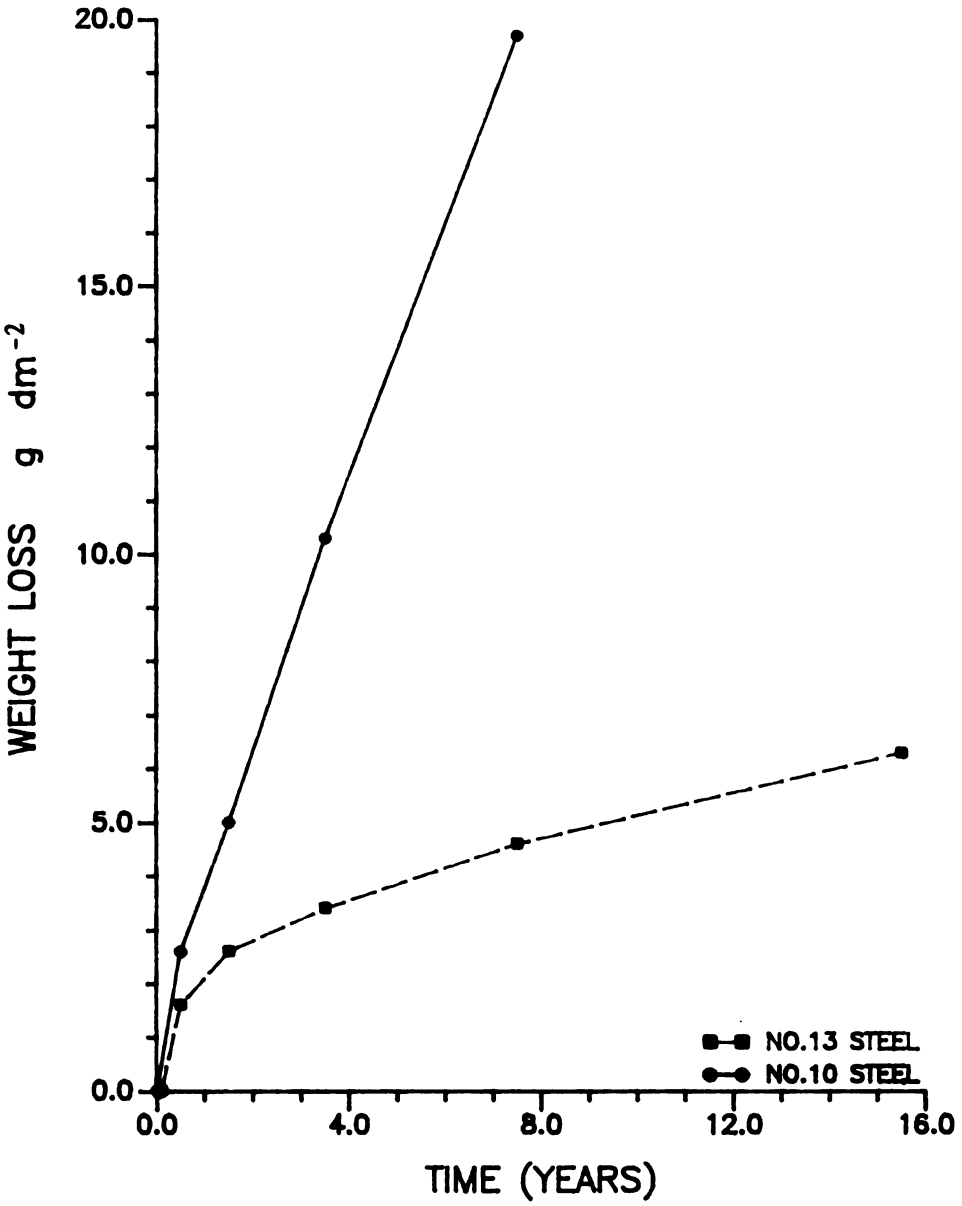

FIGURE 20. WEIGHT LOSS–TIME CURVE FOR NO.10 & NO.13 STEELS AT KURE BEACH

VI CONCLUSION:

1. When apparently identical specimens are exposed simutaneously to a corrosive environment, corrosion does not begin simutaneously. Corrosion initiations are distributed at random, and follow a Gamma function as shown by our experimental results. The parameters are fitted to each specific combination of alloy and environment.

2. Two sets of parameters were determined from the experimental results:

nails in humid air:

θ = 2.4071

R = 3.237

α = 0.

AA 2024-T3 coupons in aqueous salt immersion:

θ = 5.1191

R = 13.5918

α = 183.55.

3. "Long time" probability-damage-exposure time diagrams can be projected with 5%, 50%, 95% etc. confidence, simular to fatigue P-S-N diagrams.

4. Comparison of the power function $W = At^b$, with the

model $W = A(t-\tau)^b$ and the damage distribution hypothesis give better explaination and agreement with ASTM test data.

BIBILOGRAPHY

[1] Miller, R.N.,
private commanication, 1987

[2] Godard, H. P.
Canadian Journal of Chemical Engineering,
Vol.38 Oct. 1960, pp.167

[3] Knotkova-Cermakova, D., Bosek, B. and Vlckova, J.
"Corrosion in Natural Environments"
ASTM STP 558, 1974, pp.52-74

[4] Bragard, A.A. & Bonnarens, H. E.
""Atmospheric Corrosion of Metals"
ASTM STP 767, 1982, pp.339-358

[5] Summitt, R
"Mathematical Basis for Corrosion Prediction in
Reliability-Centered Maintainence"
NACE paper 225, 1987

[6] Williams, D.E., Westcott, C. & Fleischmann, M.
J. Electrochem. Soc., 1985 Augest pp. 1796-1804

[7] Dallek, S. & Foley, R.T.
J. Electrochem. Soc., 1976 Dec. pp.1775-1779

[8] Macdonald, D.D.
Indian J. Technol. 1986, 24(8), pp.485-491

[9] Ailor, W.H.
"Atmospheric Factors Affecting the Corrosion of Engi-
neering Metals"
ASTM STP 646 1978, pp.129-151

[10] Copson, H.R.
Proceedings, ASTM Vol.60 1960, pp.650-660

[11] Copson, H.R.
Proceedings, ASTM Vol.48 1948, pp.591-609

[12] Copson, H.R.
Proceedings, ASTM Vol.45 1945, pp.554-590

[13] LaQue, F.L.
Proceedings, ASTM Vol.51 1951, pp.495-582

[14] Copson, H.R.
Proceedings, ASTM Vol.52 1952, pp.1005-1026

[15] Little, R.E.
"Statistical Analysis of Fatigue Data"
ASTM STP 744, 1981, pp.3-23

[16] Mikhailovsky, Y.N.
"Theoretical and Engineering Principles of Atmospheric Corrosion of Metals"
"Atmospheic Corrosion" edited by Ailor, W.H.
pp.85-105

[17] Bogdanoff, J.L. and Kozin, F.
"Probabilistic Models of Cumulative Damage"
John Wiley & Sons Inc. New York, (1985)

[18] Heller, R.A. Editor
"Probabilistic Aspects of Fatigue"
ASTM STP 511

[19] Mikhailovsky, Y.N., Skurikhin, A. and Cherny, M. et al.
Zashchita Metallov, 15(5), 1979, pp.523-532

[20] Heine, M.A. and Sperry, P.R.
J. Electrochem. Soc. Vol.112 No.3 pp.359-361

[21] Bohni, H. and Uhlig, H.H.
J. Electrochem. Soc. Vol.116 No.7 pp.906-910

[22] Nguyen, T.H. and Foley, R.T.
J. Electrochem. Soc. Vol.129 No.1 pp.27-32

[23] Foroulis, Z.A. and Thubribar, M.J.
J. Electrochem. Soc. Vol.122 No.10 pp.1296-1301

[24] Strekalov, P.V., Wo, W.D. and Mikhailovsky, Y.N.
Zashchita Metallov., Vol.19 No.2 pp.220-230

[25] Guttman, H.
"Metal Corrosion in the Atmosphere"
ASTM STP 435, 1968 pp.223

[26] Mikhailovsky, Y.N. and Sokolov, N.A.
Zashchita Metallovo., Vol.18 No.5 pp.675-681

[27] Shibata, T. and Takeyama, T.
Corrosion 33 (1977) No.7 pp.243-251

[28] Filinovsky, V.Y., Dmitriev, V.I. and Strizhevsky, I.V.
Corrosion Science, Vol.25 No.2 pp.99-105

[29] Newman, J., Hanson, D.N. and Vetter, K.
Electrochemica Acta, 1977 Vol.22 pp.829-831

[30] Alkire, R.C. and Siitari, D.
J. Electrochem. Soc. Vol.129 No.3 pp.488-496

[31] Johansson, Lars-Gunner
Intl. Congress on Metallic Corrosion
(9th 1984, Toronto, Canada) Vol.1 pp.407-411

[32] Galvele, J.R.
J. Electrochem. Soc. Vol.123 No.4 pp.464-474

[33] Hebert, k. and Alkire, R.
J. Electrochem. Soc. Vol.130, No.5 pp.1007-1014

[34] Cox, D.R. and Miller, H.D.
"The Theory of Stochastic Processes"
John Weley & Sons Inc. New York, 1965

[35] Pierce, F.J.
"Microscopic Thermodynamics"
International Textbook Company, Pennsylvania, 1968

[36] Sherratt, F. and Sturgeon, J.B.
"Materials, Experimentation & Design in Fatigue"
Proceeding of Fatigue 81

[37] McGeary, F.L., Summerson, T.J. and Ailor, W.H.
"Metal Corrosion in the Atmosphere"
ASTM STP 435 pp.141-174

[38] Albrecht, P
"Probabilistic Fracture Mechanics & Fatigue Methods:
Applications for Structural Design & Maintenance"
ASTM STP 798 1981, pp.184-204

[39] Little, R.E.
"Manual on Statistical Planning and Analysis for
Fatigue Experiments"
ASTM STP 588 1975

[40] Lorking, K.F. and Mayne, J.E.O.
J. Appl. Chem. Vol.11, May 1961. pp.170-180

[41] Nguyen, T.H., Brown, B.F. and Foley, R.T.
Corrosion-Nace Vol.28 No.6 pp.319-326

[42] Pickering, H.W.
Corrosion Vol.42, No.3 pp.125-140

[43] Sweet, A.L. and Kozin, F.
J. Materials Vol.3 No.4 pp.802-823